INCORPORATION OF METAL SULFIDE CUBANES INTO FRAMEWORK SOLIDS USING N-HETEROCYCLIC CARBENES (NHCS)

by

Connor Moore

A thesis submitted to the faculty of
The University of North Carolina at Charlotte
in partial fulfillment of the requirements
for the degree of Master of Science in
Chemistry

Charlotte

2024

Approved by:

_____
Dr. Christopher Bejger

_____
Dr. Michael Walter

_____
Dr. Tom Schmedake

_____
Prof. Rachel Dickey

ABSTRACT

CONNOR MOORE. Incorporation Of Metal Sulfide Cubanes Into Framework Solids Using N-Heterocyclic Carbenes (NHCs)
(Under the direction of DR. CHRISTOPHER M. BEJGER)

Metal-sulfur cubane clusters fill an untapped niche for tunable, electrochemically active building blocks. These clusters exhibit reversible electrochemical properties and are structurally diverse. Fe_4S_4 clusters represent analogues for important biologically prevalent ferrodoxins, which perform important catalytic processes, such as nitrogen fixation in the nitrogenase enzyme. One notable goal is stabilizing these clusters due to their propensity for oxidation. We aim to utilize the characteristic stability of metal organic and covalent organic frameworks for this goal. Recent reports have shown that Janus-bis *N*-heterocyclic Carbenes (NHCs) can serve as linkers to assemble Co_4S_4 clusters. This thesis will delve into previous attempts at utilizing NHCs in the synthesis of metal sulfur cubane cluster frameworks, as well as future efforts towards this goal. Specifically, we show progress towards using covalent organic frameworks (COFs) scaffolds to anchor M_4S_4 clusters.

ACKNOLEDGEMENTS

First and foremost, I would like to thank Dr. Christopher Bejger for being my research advisor, as well as for being a mentor throughout my time as both a graduate student, as well as an undergraduate student. My time in your lab has been immeasurable due to the vast amount of experience I have received.

I would also be remised if I did not also thank fellow graduate student Jonathan Gillen for both taking me under his wing when I was an undergraduate student, as well as for providing insight into proper procedures. You also graciously took time out of your busy schedule to run PXRD, SEM, and EDAX, and for that I thank you. I would also like to thank fellow graduate student Hasan Fuead, you have helped me to be a better person. Thank you to both Jonathan and Hasan for making the lab a continued joy to work.

Thank you to all my committee members: Dr. Michael Walter, Dr. Tom Schmedake, and Prof. Rachel Dickey, who helped provide outside opinions. I would also like to thank Dr. Adam Fessler for providing insight on intricacies of analytical instruments and answering any NMR questions I came to him with. I would like to acknowledge the various people who have helped me collect PXRD data for analysis whether that be my Dr. Natalia Shushtova at the University of South Carolina, Dr. Akhilesh Tripathi at Rigaku Americas, or Dr. Diane Dickey at the University of Virginia.

Lastly, I would like to thank my family for pushing me forward, even when I may not have wanted to. I would like to thank my mother Krista, and my aunt, Ann. Without you all I may not have endured this endeavor.

TABLE OF CONTENTS

LIST OF FIGURES

LIST OF SCHEMES

LIST OF ABBREVIATIONS

1D	One-Dimensional
^{1}H NMR	Proton Nuclear Magnetic Resonance
^{31}P NMR	Phosphorous Nuclear Magnetic Resonance
AmCOF	Amide Covalent Organic Framework
BFMBIM	4,7-bis(4-formylbenzyl)-1-methyl-1H benzimidazole
BoCOF	Benzoxazole Covalent Organic Framework
COF	Covalent Organic Framework
DCM	Dichloromethane
DMC	Dimethyl Carbonate
DMSO	Dimethyl Sulfoxide
EPR	Electron Paramagnetic Resonance
HCl	Hydrochloric Acid
IR	Infrared
KO^{t}Bu	Potassium tert-butoxide
$LiAlH_4$	Lithium Aluminum Hydride
MCOP	Main Chain Organometallic Polymer
MeCN	Acetonitrile
MeOH	Methanol
MOF	Metal Organic Framework
n-BuOH	*n*-Butanol

NaOH	Sodium Hydroxide
NHC	*N*-Heterocyclic Carbene
o-DCB	ortho-Dichlorobenzene
PSM	Post-Synthetic Modification
PTA	1,3,5-triaza-7-phosphaadamantane
PXRD	Powder X-Ray Diffraction
RT	Room Temperature
SEM	Scanning Electron Microscopy
THF	Tetrahyrofuran

CHAPTER 1: INTRODUCTION

1.1 Metal Sulfur Compounds

Metal sulfur compounds are observed in many forms of nature, with one of the most notable examples of their utility being the crucial role they play in the enzyme nitrogenase. Nitrogenase, an enzyme responsible for the ATP-dependent reduction of N_2 to NH_3, consists of three metal sulfur clusters: an Fe_4S_4 cluster, Fe_8S_7 cluster, and a $MoFe_7S_9C$ cluster. N_2 by itself is a fairly unreactive chemical species, and so, it is imperative to transform it into its much more useful form of nitrogen, NH_3. Nitrogenase is comprised of two distinct proteins, each of which contains metal sulfide clusters, with one functioning as the electron carrier and one as a catalyst (Figure 1.1). The Fe protein within the Mo-nitrogenase contains multiple ATP binding sites; once ATP is bound, the Fe protein associates with the MoFe protein, allowing for nitrogen fixation to occur. Then, the Fe_4S_4 cluster abstracts electrons from the ATP binding site where it is translocated from the Fe protein to MoFe cluster via the Fe_8S_7 cluster, from which it is finally transferred to the $MoFe_7S_9C$ cluster to participate in the reduction of N_2 into NH_3.[1]

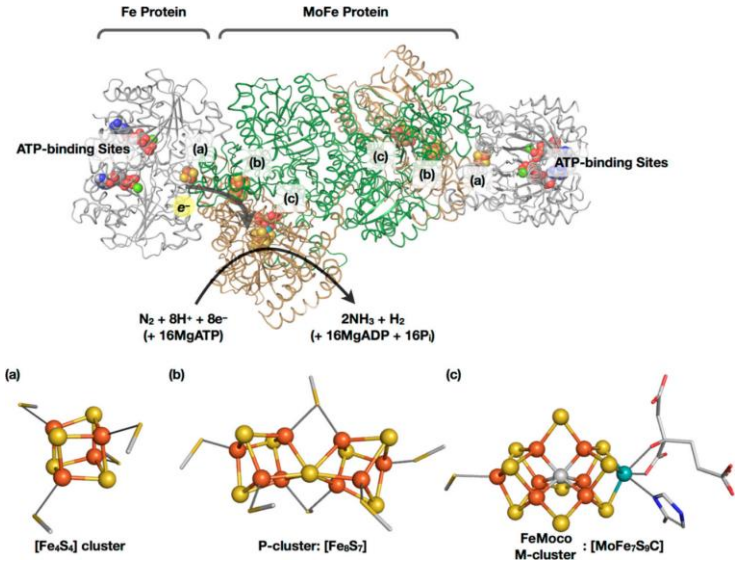

Figure 1.1. A diagram of nitrogenase, highlighting the roles of the three metal-sulfide clusters in the reduction of N_2 to NH_3. (Reprinted with permission from Figure 1 Copyright 2020 American Chemical Society.)

Another example of these metal sulfur compounds in nature would be magnetotactic and sulfate reducing bacteria. These bacteria produce iron sulfite minerals such as greigite ($Fe^{2+}Fe^{3+}S_4$) and are found in hydrothermal vents.[2] Pyrite, which is commonly found in volcanic environments, also has potential ties to life. Due to their extreme temperature and pressure, volcanoes have been proposed as one of the possible birthing places of life. Günter Wächtershäuser proposed just this with his "Iron Sulfur World Hypothesis" in 1992.[3] He hypothesized that the surface of pyrite acts as a reaction surface where reductive carbon fixation can occur, and thus mimics growth we see today. As these ligands are forming, they are initiating an autocatalytic feedback process which could constitute reproduction (Figure 1.2). Lastly, a method of evolution was proposed with the term "double feedback". Double feedback is the process by which a pathway branches, and with this branching a previous step is weakened due to intermediates and

Le Chatelier's principle. This, combined with the autocatalytic feedback process, meant certain pathways were favored over others.[4]

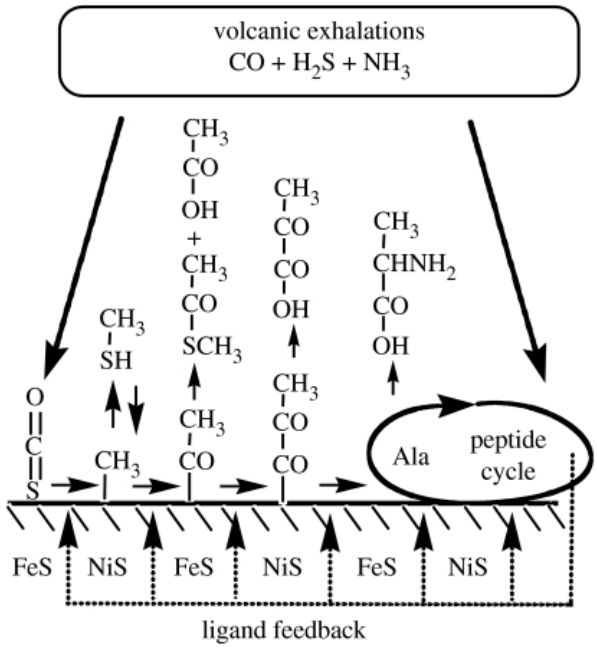

Figure 1.2. A diagram showcasing an example of the proposed autocatalytic feedback process. (Reprinted with permission from Figure 3 Copyright 2006 The Royal Society)

1.2 Metal Sulfide Cubanes

Synthetic versions of Fe_4S_4 clusters are highly desirable due to their chemical tunability, electrochemical properties, and possible applications in catalysis. The Holm laboratory has prepared a number of such clusters that are isostructural and isoelectronic to the naturally occurring iron-sulfur cubanes (Figure 1.3).[5] One of the key challenges that arises from working with these clusters is their sensitivity towards oxidizing impurities.

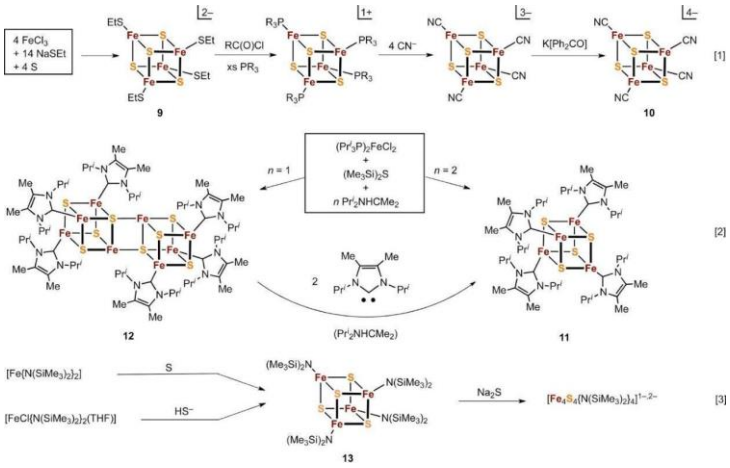

Figure 1.3. Scheme showcasing the many ways that the Fe_4S_4 cluster could be altered and how these affected core properties of the cluster. (Reprinted with permission from Figure 3 Copyright 2014 American Chemical Society.)

Many synthetic analogues for the $Fe_4S_4^{3-,2-,1-}$ have been isolated and studied; however, the existence of the $Fe_4S_4^{0}$ remained speculative for decades. In fact, nitrogenase was believed to only utilize the $Fe_4S_4^{1+/2+}$ redox couple until the mid 1990's. However, in 1994 it was discovered that the so called all-ferrous $Fe_4S_4^{0}$ is also present. This was shown utilizing oxidative electron paramagnetic resonance (EPR) titration to track the decomposition of the Fe_4S_4 cluster with bipyridine under anaerobic conditions and no additional reductants added. It was found that >97% of the Fe released was in the Fe^{2+} form. When compared to the control, $Fe_4S_4^{1+}$ cluster, which produced only a small amount of Fe^{2+} it was apparent that the Fe_4S_4 cluster must be present in the neutral form.[6] Holm's group was also the first to isolate the neutral form utilizing the electron donating prowess of *N*-heterocyclic carbene (NHC) ligands (Figure 1.4). The $Fe_4S_4(Pr^i{}_2NHCMe_2)_4$ was characterized *via* various methods including single crystal X-ray diffraction, cyclic voltammetry, as well as ^{1}H NMR, Mössbauer, and absorption spectroscopies. With that

being said, the isolation of the Fe_4S_4 cluster remains challenging, due to its propensity to aggregate to the $Fe_{16}S_{16,}$ or the Fe_8S_8 cluster.[7]

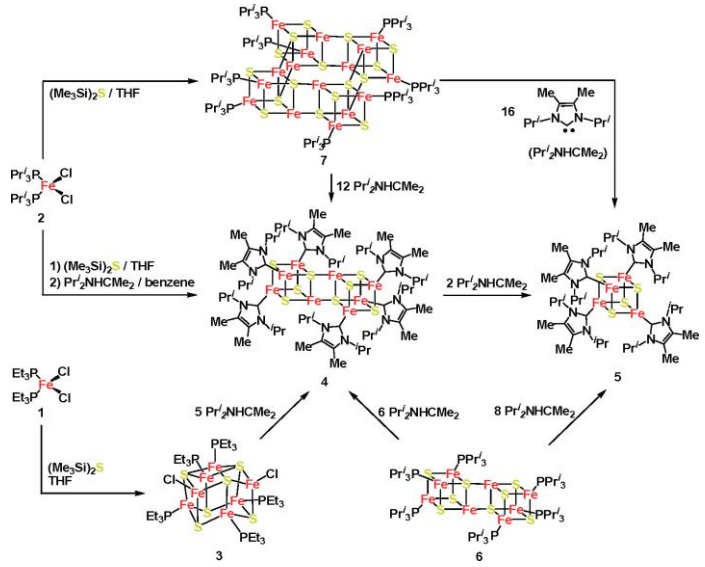

Figure 1.4. Scheme showing the reaction pathway for forming the Fe_4S_4 cluster. (Reprinted from Figure 1 Copyright 2008 American Chemical Society.)

Other M_4S_4 clusters composed of different transition metals have also been reported. For example, the Co_4S_4 cluster with NHC ligands is the first non-iron transition metal cluster to exhibit cubane topology. Additionally, it has similar redox capabilities and magnetic ground states as the Fe_4S_4 cluster (Figure 1.5). The Co_4S_4 cluster is consistent with the Fe_4S_4 in its favorability for NHCs over phosphine ligands, further cementing the idea of NHCs being better electron donors.[8]

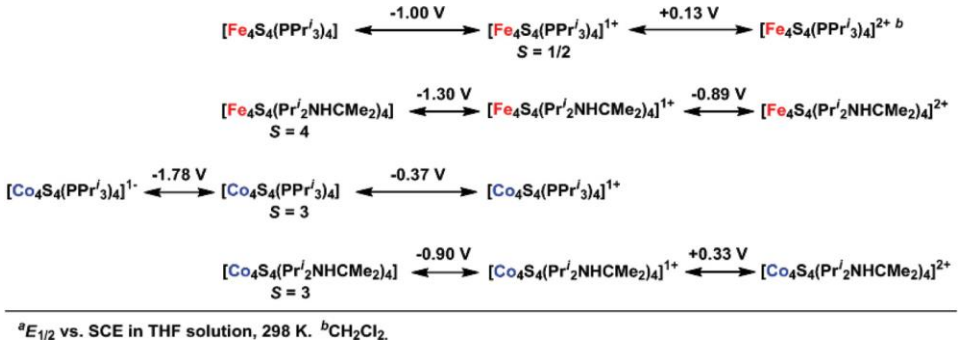

Figure 1.5. Redox Potentials of the Fe_4S_4 cluster and the Co_4S_4 cluster. (Reprinted from Figure 7 Copyright 2009 American Chemical Society.)

1.3 Metal Sulfide Cubane Cluster Materials

The aforementioned clusters can be integrated into material frameworks to achieve crystallinity, dimensionality, and stability required for potential applications. Many research groups have attempted to prepare materials from these discrete cluster precursors. However, it remains a challenge to prepare M_4S_4-based frameworks that are porous, crystalline, and stable. Kanatzidis's group utilized a dual-metal sulfide cluster chalcogel, containing both the previously mentioned Fe_4S_4 cubane cluster and a Sn_4S_{10} cluster, for the purpose of hydrogen evolution in the presence of a ruthenium dye. Being a chalcogel, this material was exceptionally porous, and thus had excellent surface area. However, the inorganic chalcogel is not crystalline (Figure 1.6).[9] Crystallinity is important due to the fact that it guarantees minimal defects. Crystallinity ensures the constraint of repeating unit cells, leading to increased atomic precision. Crystallinity allows for understanding where the atoms are, and as such, allows for a better structure-function understanding and modeling for potential catalytic applications.

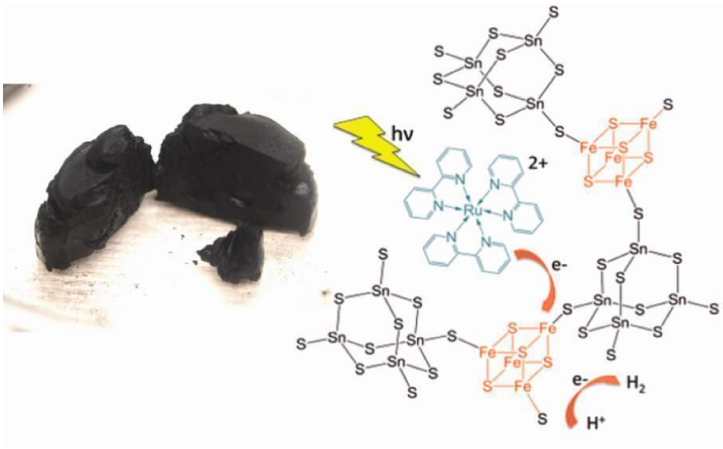

Figure 1.6. Image of Kantzidis's chalcogel, the chemical structure, and its reaction with light. (Reprinted with permission from Abstract Copyright 2013 American Chemical Society.)

While the Kanatzidis group had issues with crystallinity, other research groups, such as the Anderson laboratory, have reported a material with excellent crystallinity. They employed the use of benzenedithiol ligands to link the discrete Fe_4S_4 cluster into a one-dimensional (1D)-coordination polymer. Anderson's group showed that crystalline materials of the discrete cluster were obtainable *via* tunability of the ligands, while also retaining the cluster's signature electrochemical properties (Figure 1.7).[10] However, due to the limitations of surface area that accompany 1D-materials, new synthetic strategies are needed.

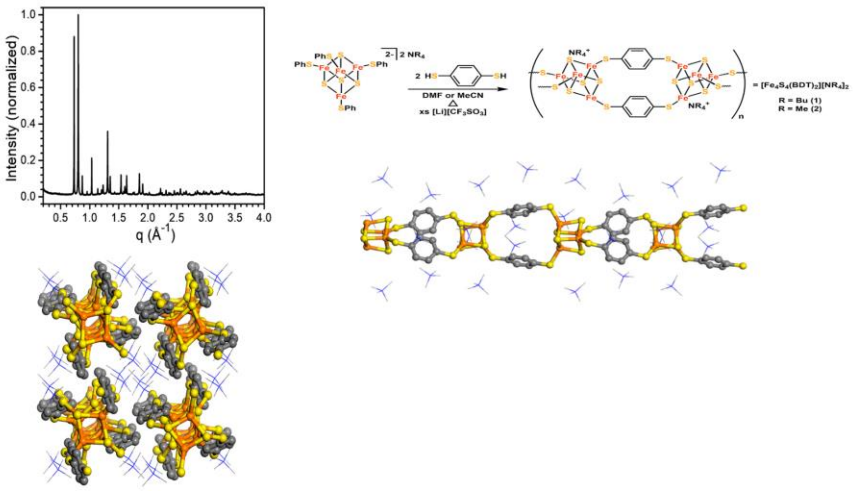

Figure 1.7. Anderson's 1-D Coordination Polymer. (Reprinted with permission from Figure 2 Copyright 2019 American Chemical Society.)

The unique redox properties of the Fe_4S_4 cubane cluster are preserved in these materials; however, neither material achieved both high surface area and crystallinity. The goal of this thesis is to propose methods for achieving the crystallinity of Anderson's coordination polymer and the porosity of Kanatzidis's chalcogel through the use of covalent organic frameworks (COFs) and metal organic frameworks (MOFs).

1.4 Metal Organic and Covalent Organic Frameworks

A metal-organic framework (MOF) is defined as a coordination network comprising metal clusters crosslinked by organic ligands and containing potential voids or pores.[11] Research into MOFs has been blossoming due to their high chemical and thermal stability, porous structure, and highly customizable nature (Figure 1.8).[12]

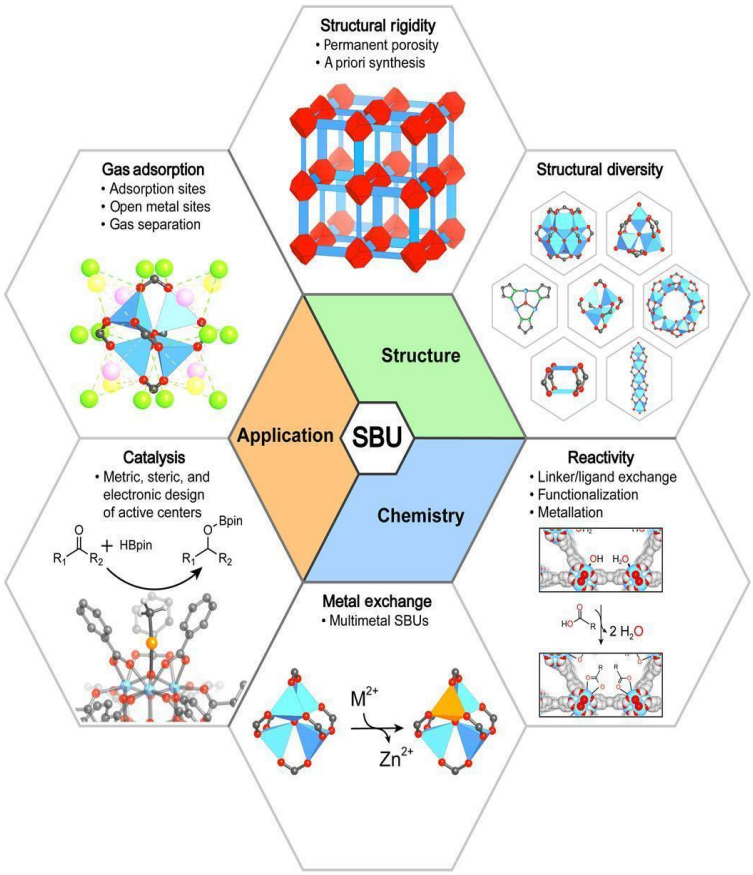

Figure 1.8. Overview of the customizability, and diversity of MOFs, as well as possible applications. (Reprinted with permission from Fig. 1 Copyright 2018 The American Association for the Advancement of Science.)

Covalent-organic frameworks (COFs), on the other hand, are frameworks of entirely organic molecules covalently bonded together. COFs enjoy higher chemical and thermal stability than MOFs but exhibit lower crystallinity. Part of the reason COFs are less crystalline is because they employ the use of covalent bonds instead of the coordination bonds found in MOFs; this leads to them having greater stability at the cost of crystallinity. This is because the more reversible a reaction, the greater the chance that defects in the structure are replaced and fixed, and coordination bonds are inherently more reversible.

Just as MOFs are made up of many different metals, COFs are also composed of multiple classes of linkages. Most commonly COFs are composed of boronate esters, imines, alkenes, and imides, which are formed *via* condensation reactions. One of benefits of COFs is that they are comprised of entirely organic molecules and covalent bonds (Figure 1.9).[13]

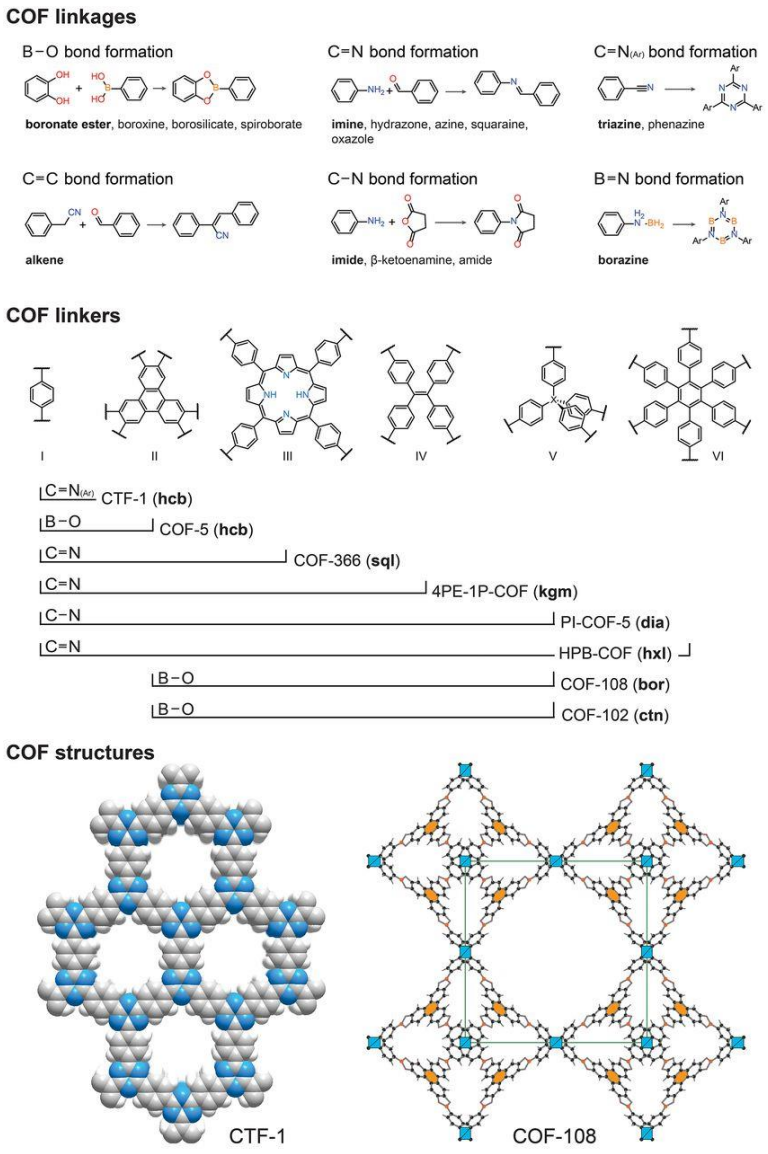

Figure 1.9. Figure showcasing various COF linkages and structures. (Reprinted with permission from Fig. 3 Copyright 2017 The American Association for the Advancement of Science.)

This allows for the manipulation of an entire framework as one large molecule. One could then modulate it accordingly, either pre- or post-synthetically to fit their needs. This tunability is intrinsic to COFs and MOFs in part because there are multiple variations, allowing for niche specific modifications.

Often compared to zeolites for applications sake,[14] MOFs and COFs both have the benefit of tunable pore size, and the ability to be post-synthetically functionalized. One of the most common proposed applications for framework materials would be that of gas storage due to the pore volume and surface area. As atmospheric CO_2 levels rise and searches for alternative fuel sources, such as H_2, become more prominent on the global stage, materials to store these gasses is becoming a growing field of research. The applications of MOFs and COFs extend beyond gas storage. For example, these crystalline frameworks can also be used for energy storage and catalytic applications.[15] Other possibilities include drug delivery vehicles.[16] The tunability of these framework materials is crucial for medical applications. For example, there are some arsenic compounds, which while harmful in certain aspects, have also been shown to be effective when combating certain illnesses, and it has been shown that MOFs and COFs could be loaded with the desired drug, and then functionalize it in such a way to release the drug in the correct area of the body.[17]

However, one of the main differences between MOFs and COFs, besides the obvious presence of metals or not, is the diversity of synthesis pathways that exist for forming MOFs as compared to that of COFs. MOFs are generally synthesized by one of five main routes: solvothermal, mechanochemical, microwave assisted, electrochemical,

or sonochemical.[18] COFs are traditionally formed under solvothermal conditions through condensation reactions. These synthetic constraints, coupled with the fact that COFs are less likely to be crystalline when compared to MOFs, are some of the main reasons why MOFs have received more attention in recent years.

CHAPTER 2: STPEWISE SYNTHESIS OF MOFS AND ORGANOMETALLIC POLYMERS

2.1 The Molecular Cluster Approach

The Bejger research group has prepared hybrid MOF-materials from discrete, metal-sulfur, molecular cluster precursors. Freeman and colleagues were able to achieve single crystal XRD data for a multi-cluster MOF using a stepwise approach. A stepwise approach was employed due to the challenge they faced from using metal sulfur clusters. Traditional multi-cluster frameworks utilize much simpler metal oxide clusters. With the knowledge that phosphorus containing groups had been used in MOF construction, phosphine linkers were employed,[19] allowing for the successful synthesis of a crystalline framework consisting of both a Co_6Se_8 cluster and a Cu_4I_4 cluster linked together by the phosphine group 1,3,5-triaza-7-phosphaadamantane (PTA). Notably this reaction took place as a stepwise approach, as opposed to a one-pot reaction, to ensure the two metallic clusters formed properly and bonded with correct orientation (Figure 2.1).[20]

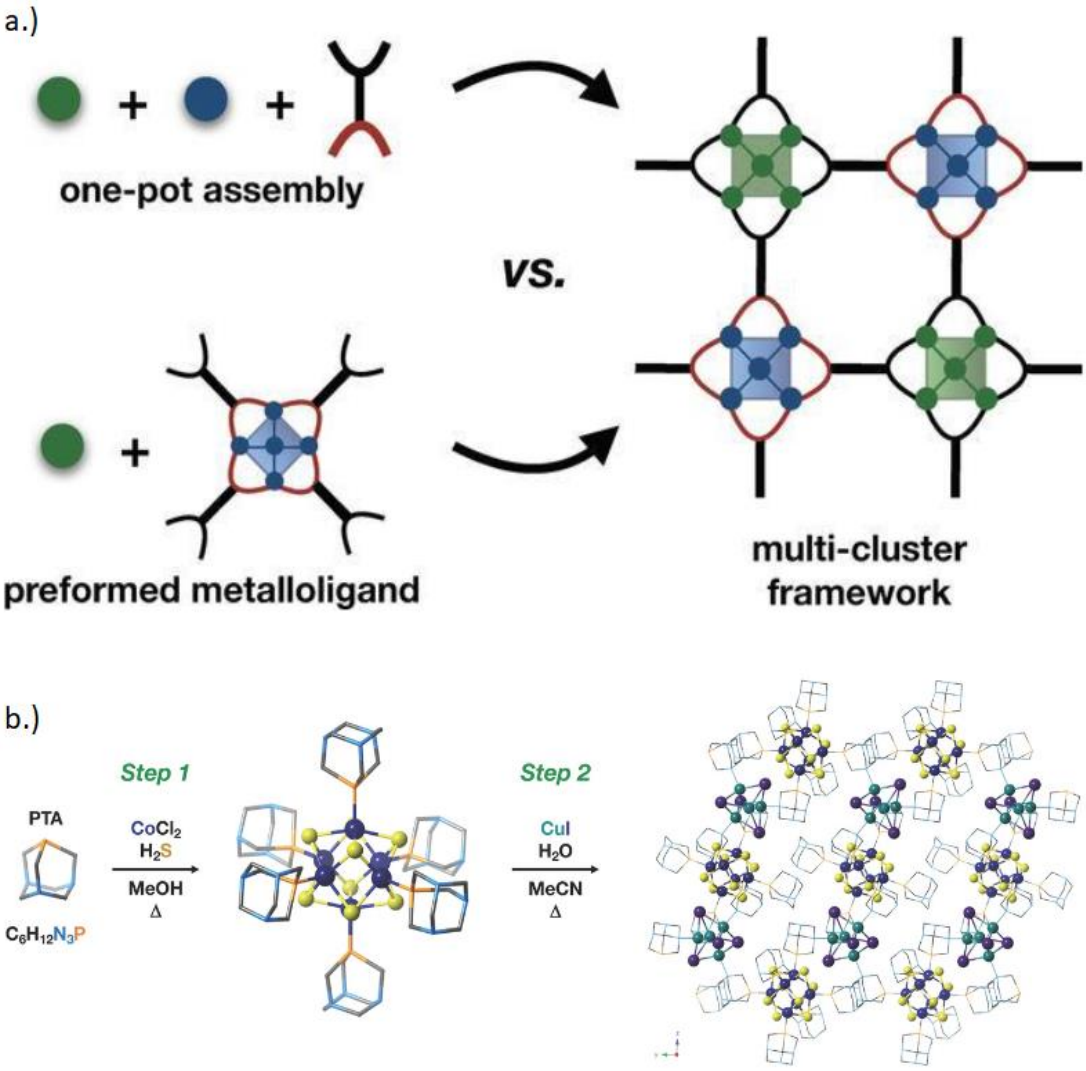

Figure 2.1. a.) Representation of why stepwise approach was needed in the formation of a multi-cluster framework. b.) Scheme for the synthesis of the multi-cluster framework. (Reprinted with permission from Figure 1 and Scheme 1 Copyright 2020 Wiley-VCH GmbH).

This framework was shown to have the band gap of an optical semiconductor as well as reversible redox chemistry when used to modify electrodes. Nonetheless, this framework is not porous, due to the angle between the phosphorus and nitrogen atoms in the PTA ligands.

My early work in the Bejger laboratory focused on modifying Co_4S_4 clusters with NHC ligands, based on the Holm approach of phosphine ligand substitution reactions. The Co_4S_4 cluster was chosen due to its structural integrity during substitution. Specifically, it remains the Co_4S_4, and does not undergo core aggregation. Attempts were made to utilize dual-faced "Janus" NHCs to link the clusters into a crystalline framework. Unfortunately, production of a crystalline material was unsuccessful, and all efforts yielded a mostly amorphous polymer dubbed main chain organometallic polymer (MCOP) (Figure 2.2). Unrelenting, we proceeded to analyze and characterize this polymer and noticed that properties of the cluster remained, insinuating that the cluster was still intact. We also made efforts to modulate the synthesis by utilizing mono-NHCs for digestion. The mono-NHCs have a higher binding affinity with the cluster, and as such, disassemble the MCOP, and extract the cluster as $Co_4S_4(^iPr_2NHCMe_2)_4$.[21]

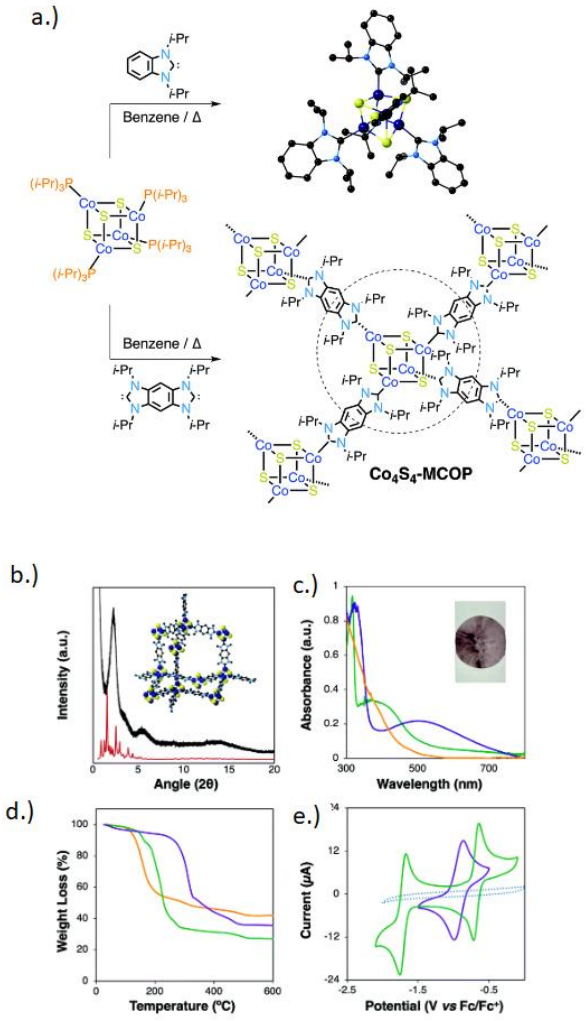

Figure 2.2. a.) Scheme for synthesis of MCOP, b.) Synchrotron powder X-ray diffraction pattern of Co_4S_4-MCOP (black) and simulated pattern (red) of model (inset), c.) normalized UV-vis absorption spectra (inset image of Co_4S_4-MCOP in epoxy) and d.) TGA traces of Co_4S_4-MCOP (purple), $Co_4S_4(^iPr_2NHCMe_2)_4$ (green), and $Co_4S_4(^iPr_3P)_4$ (orange), and e) cyclic voltammograms of Co_4S_4-MCOP (purple; solid-state modified glassy carbon working electrode), $Co_4S_4(^iPr_2NHCMe_2)_4$ (green), and background (blue dashed). Recorded at 100 mV s^{-1} in MeCN with $TBAPF_6$. (Adapted from Scheme 1 and Figure 1 2022 Royal Society of Chemistry.)

2.2 Stepwise Approach

Carboxylates are a known linker for MOFs containing Zn^{2+}, Cu^{2+}, and Zr^{2+}.[22] We propose the backside functionalization of benzannulated NHCs as linkers between the

Co_4S_4 cluster and one of the metals in the synthesis of framework materials (Figure 2.3). It is known in the literature that similarly functionalized NHCs are used to stabilize other discrete clusters, such as Au nanoparticles.[23]

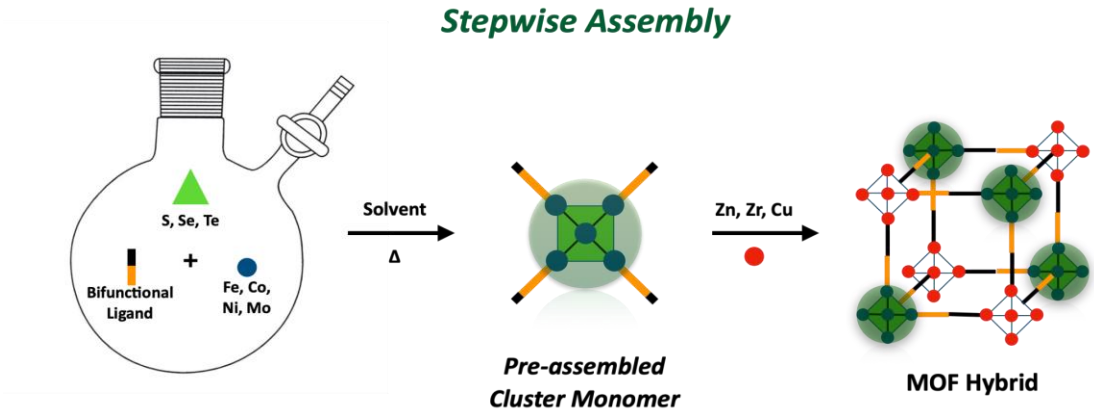

Figure 2.3. Proposed pathway for utilizing NHCs in the formation of MOFs.

With the goal of producing carboxylate NHCs, three main avenues were explored (Figure 2.4).

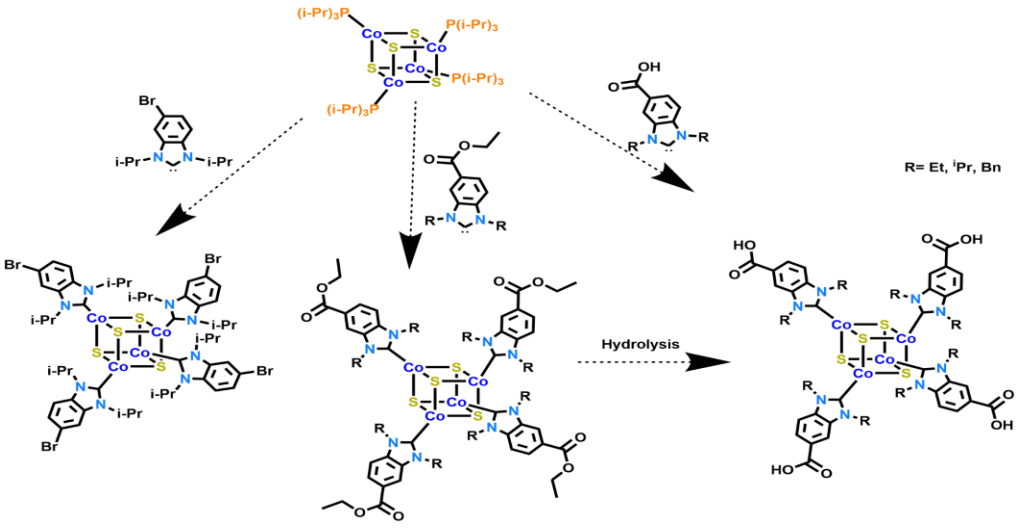

Figure 2.4. Proposed routes for utilizing functionalized benzannulated NHCs.

Two routes started with 5-benzimidazole carboxylic acid (**1***)* as a precursor. Esterification of the acid was used to protect it during *N*-alkylation with either benzyl bromide,[24] ethyl bromide,[25] or isopropyl bromide.[23] Alkylating agents were selected based on ease of use, as well as steric hindrance. Isopropyl bromide, while the most sterically bulky, was significantly harder to alkylate with when compared to the ethyl bromide reagent (Scheme 2.1).

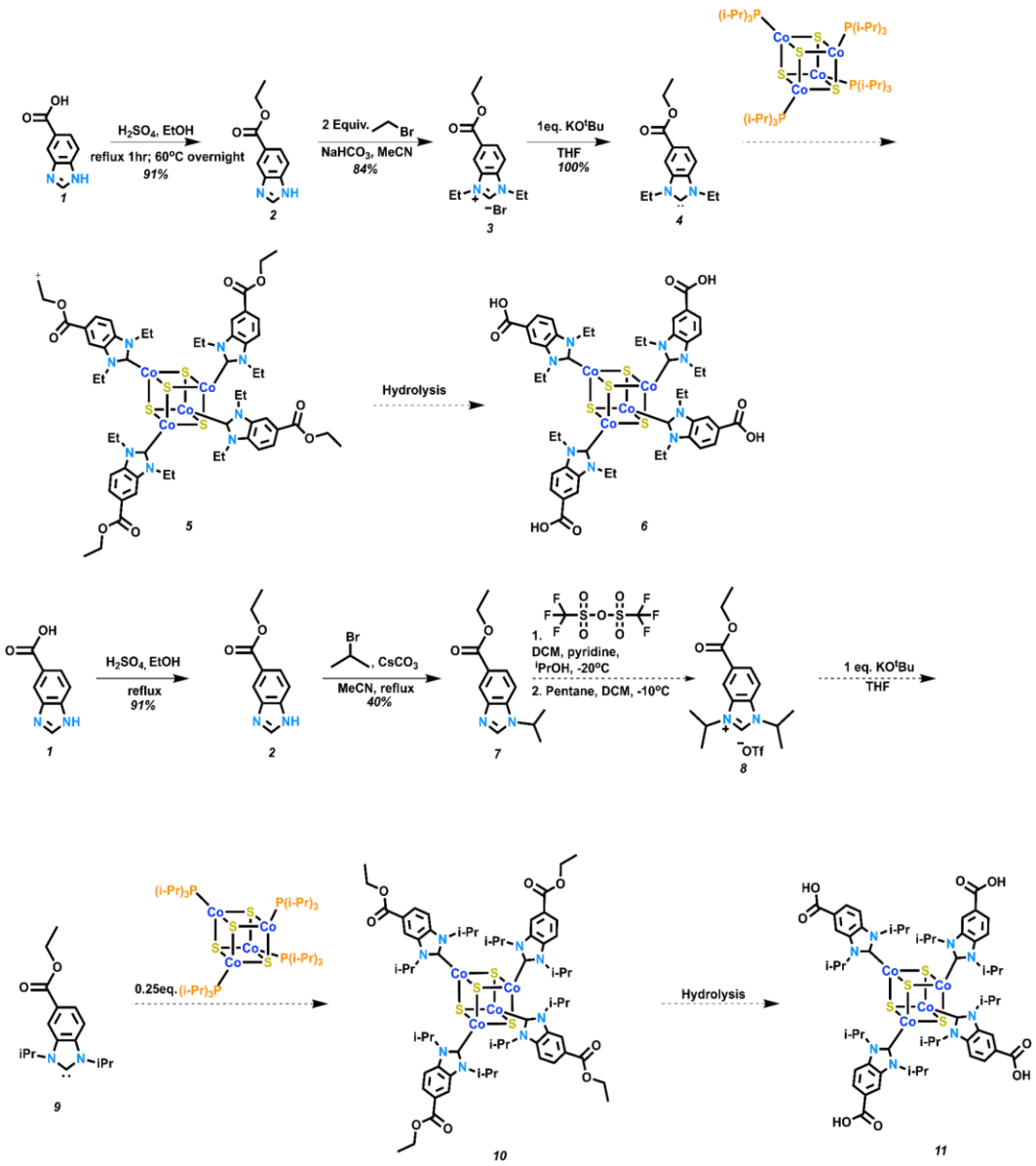

Scheme 2.1. Proposed scheme for synthesis of MOF using carboxylate functionalized NHC.

We explored two options to prepare the fully substituted NHC cluster after formation of the fully alkylate imidazolium was isolated. The first option involved immediate formation of the NHC *via* deprotonation (**4, 9**), followed by adduction onto the $Co_4S_4(^iPr_3P)_4$ cluster. However, one concern that arose during our endeavors was that of

the Co_4S_4 cluster's stability during the hydrolysis of the ester back to a carboxylic acid. Due to this concern, we also explored hydrolyzing the ester prior to addition of the NHC to the cluster, leading to the formation of a novel zwitterionic NHC precursor (**15*)*** (Scheme 2.2).

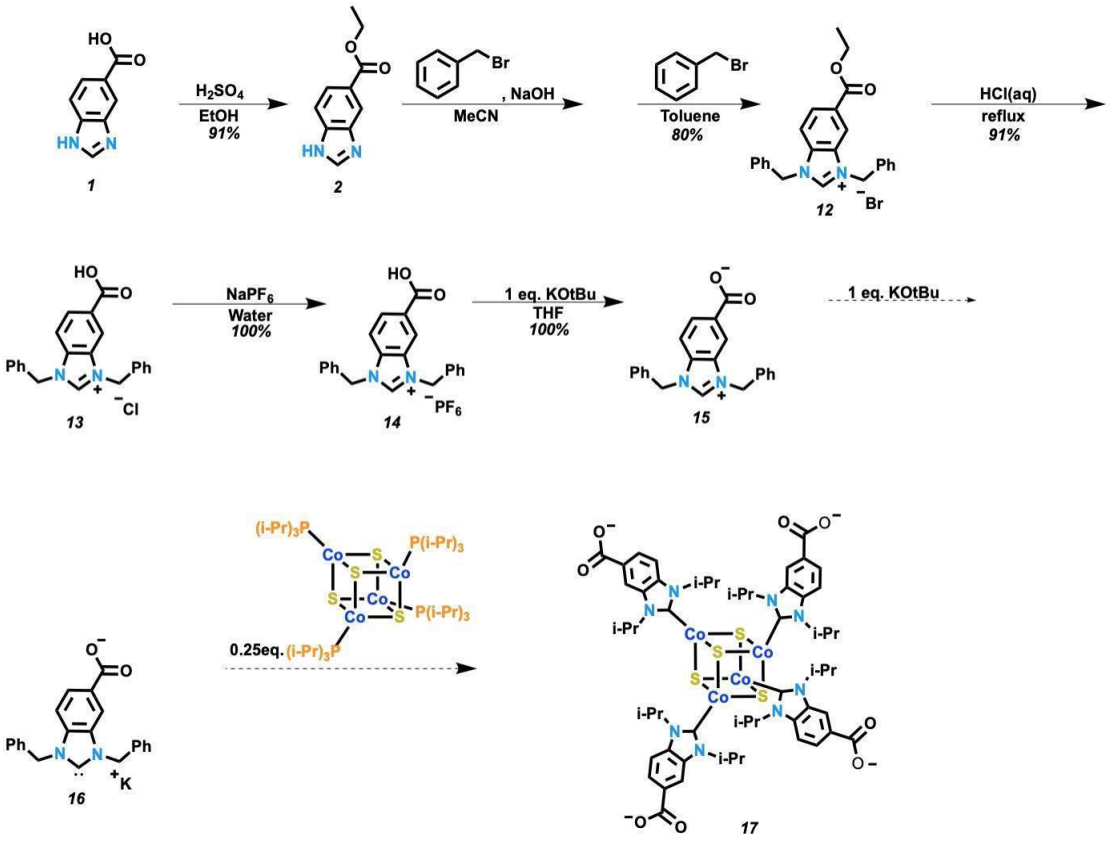

Scheme 2.2. Proposed scheme for synthesis of MOF using zwitterionic intermediate.

Problems arose when crystallization was unsuccessful after addition of the cluster. We theorize that this was likely the result of incomplete displacement of the phosphine ligands, or potential dimerization leading to an impure product. Thus, we attempted to use functionalized NHCs prepared with 5-bromo benzimidazole (**18**),[26] from which alkylation was immediately available. Once alkylated (**19**), deprotonation and phosphine

displacement were attempted, at which point a lithium halogen exchange followed by a carboxylation reaction would be performed. Once transformed into a carboxylic acid (**22**), reaction with $Zn(NO_3)_2$ would likely result in MOF completion (Scheme 2.3).

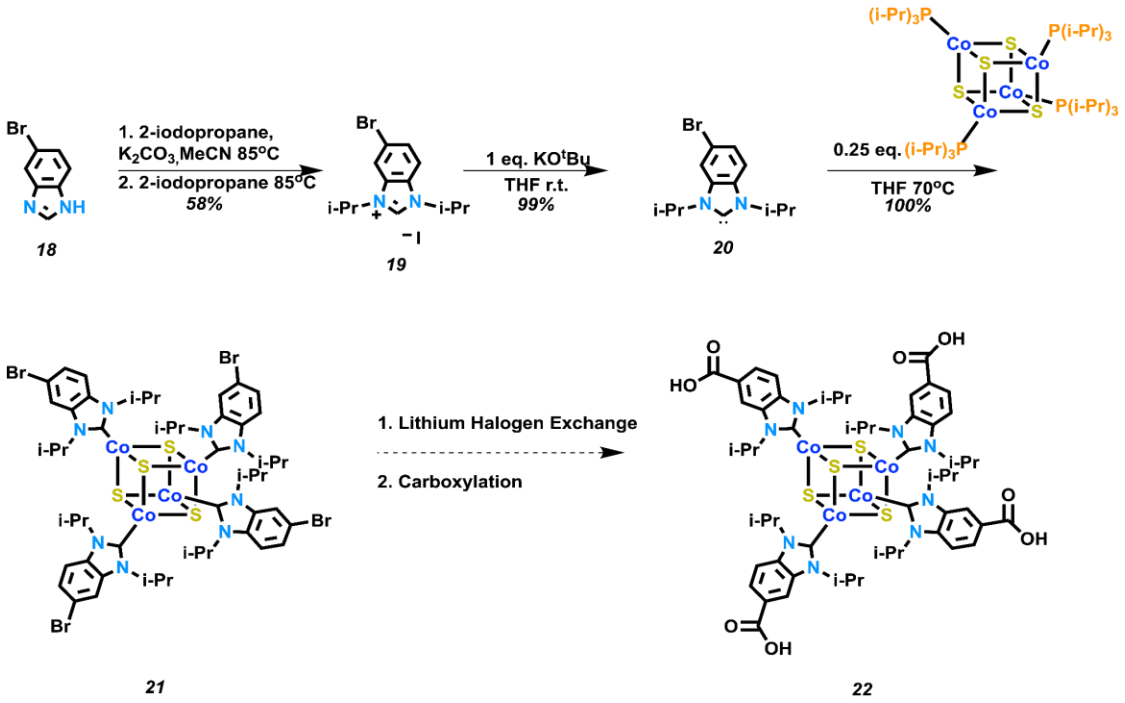

Scheme 2.3. Proposed scheme for synthesis of MOF using bromine functionalized NHC.

These methods provide insight into the challenges of using NHCs to displace the phosphine ligands of the Co_4S_4 cluster even though they were unsuccessful. Displacement of the phosphine ligands was confirmed via ^{1}H NMR and ^{31}P NMR spectroscopy analysis. The -CH proton present in the $Co_4S_4(^iPr_3P)_4$ cluster exhibits a distinct chemical shift around 14.7 ppm in ^{1}H NMR spectroscopy. Addition of **20**, and the subsequent displacement of the triisopropylphosphine ligands leads to an observed shift of this peak. We did not observe any recognizable peaks in the ^{31}P NMR-spectrum when analyzing the Co_4S_4 cluster. However, once exposed to the various NHCs, the

signal for free $^{i}Pr_3P$ was observed around 20 ppm, indicating that displacement has taken place. However, the ^{1}H NMR spectra is inconclusive due to the shift of this peak at approximately 12 ppm. We would expect to observe 2 peaks in this region, one from the carboxylic acid, and another from the carbene's alkyl groups (Figure 2.5). All of this, combined with inability to recrystallize the product and its appearance as oil lead to the conclusion that the product was impure. This coupled with cyclic voltammetry showing no redox activity indicated further purification methods would need to be investigated.

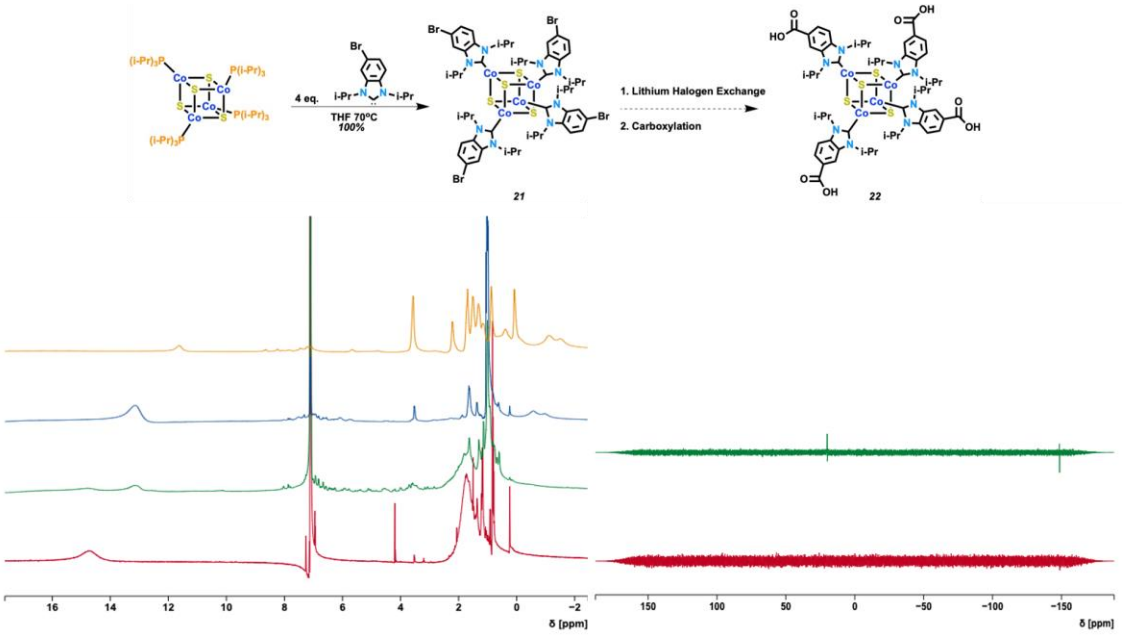

Figure 2.5. ^{1}H NMR and ^{31}P NMR spectra showcasing the addition of **20** to $Co_4S_4(^{i}Pr_3P)_4$ and the subsequent formation of **22** via carboxylation of **21** along with an accompanying scheme of this reaction. Red = $Co_4S_4(^{i}Pr_3P)_4$; Green = **21** partial displacement Blue = **21** full displacement; Orange = **22**

CHAPTER 3: POSTSYNTHETIC MODICATION OF COFS

3.1 COF Scaffolding

We also aim to utilize a preformed framework, such as a COF, as a scaffold to stabilize the Co_4S_4 cluster. We propose this method due to the hope that the crystalline nature will be retained post modification. One related example of post-synthetic modification (PSM) of a framework from the literature was the addition of hydrogenase active sites, composed of a Fe_2 cluster, to UiO-66 (Figure 3.1). The [FeFe](bdt)$(CO)_6$ cluster has been shown to be a catalyst for proton reduction catalyst with electrochemical and photochemical capabilities; however, it is thermally unstable.[27] UIO-66 is thermally stable, and so PSM allows for this stability to be applied to the cluster. The Fe_2 cluster's coordination within the framework was confirmed via X-Ray Absorption Spectroscopy. This hybrid material was also found to be an effective catalyst with a $[Ru(bpy)_3]^{2+}$ dye as an electron donor in photochemical arrays.[28]

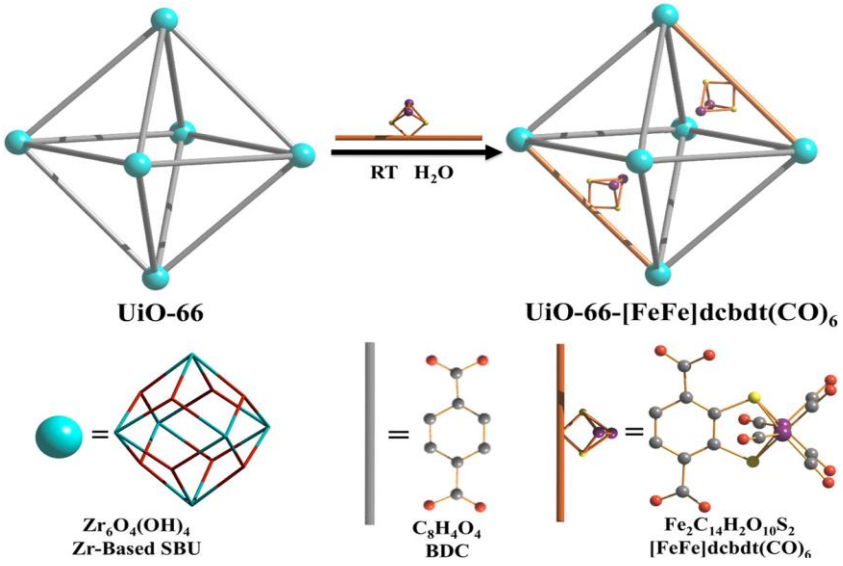

Figure 3.1. Representation of post-synthetic exchange of [FeFe](bdt) into the UIO-66 framework. (Reprinted with permission from Figure 2 Open Access Copyright 2013 American Chemical Society.)

3.2 NHC COFs

We considered two approaches to anchor clusters to the interior pores of COFs (Figure 3.2).

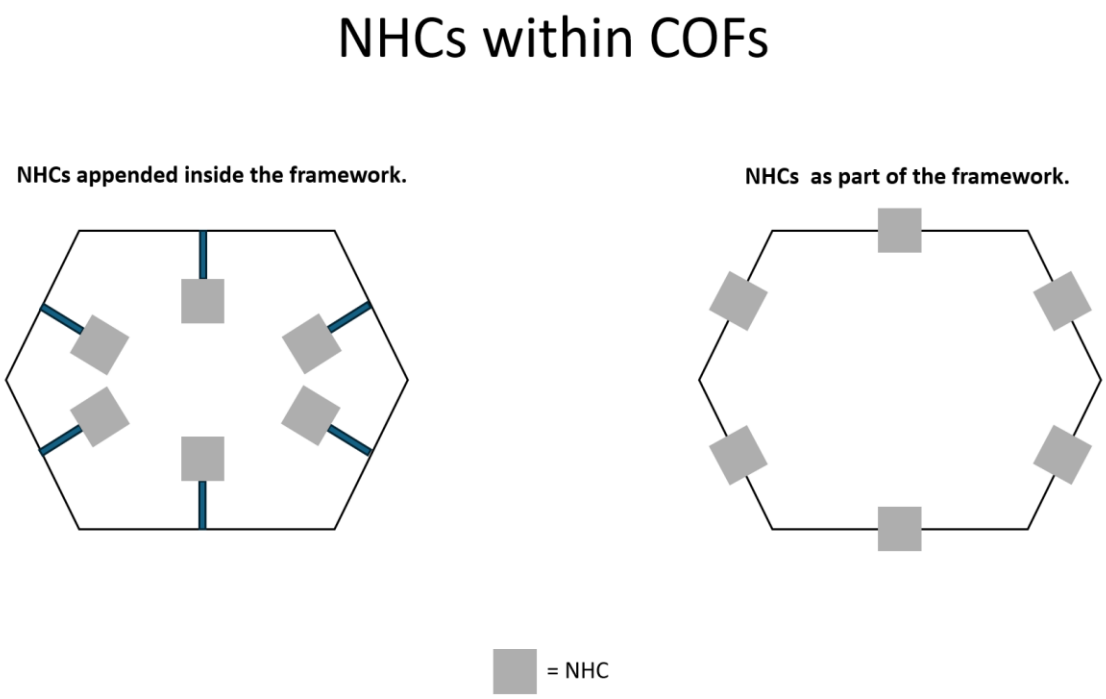

Figure 3.2. Graphical representation of the two types of NHC COFs.

First, we explored the post-synthetic addition of NHCs inside COFs[29]. We also prepared COFs with NHCs already present in the pore walls. The former requires additional consideration with respect to pore size to ensure adequate space for the cluster is present in the pore. For this reason, COFs with NHCs already present in the pore walls are more common. Both of these types of NHC COFs are desirable for NHCs' ability to capture CO_2 in an elegant manner.[30] The NHC binds to the CO_2 readily, and releases the CO_2 in the presence of heat, allowing for situational access to either CO_2 or the NHC. It has also

been shown that the CO_2 can go through an electrochemical reduction process and power an H-type cell in imidazolium COFs.[31]

3.3 Challenges with COFs

Special attention must be made towards ensuring that pore size is suitable for habitability of an M_4S_4 cluster. Consideration must be made for either lack of size or interpenetration of the crystal structure. One must also ensure that X-ray diffraction instruments capable of low 2θ are employed in characterization due to the large spacing present due to the pores. Another concern that arises from handling these framework materials is ensuring that the crystal integrity remains intact. Supercritical CO_2 is sometimes used in the literature to prevent structural collapse upon solvent removal. Other approaches propose a "gentle nitrogen method" wherein the solvent is repeatedly exchanged to a lower surface tension solvent, tetrahydrofuran > methanol > dichloromethane > *n*-hexane, and then the material is heated under a continuous, gentle stream of N_2 as a substitute for supercritical CO_2.[32]

3.4 Frameworks Functionalized with NHCs

My work began with the investigation and synthesis of COF-HNU3 (Scheme 3.1).[29] Due to the cost of purchasing the starting material, efforts were made to synthesize 2-hydroxyterepthalaldehyde (**23**) instead.

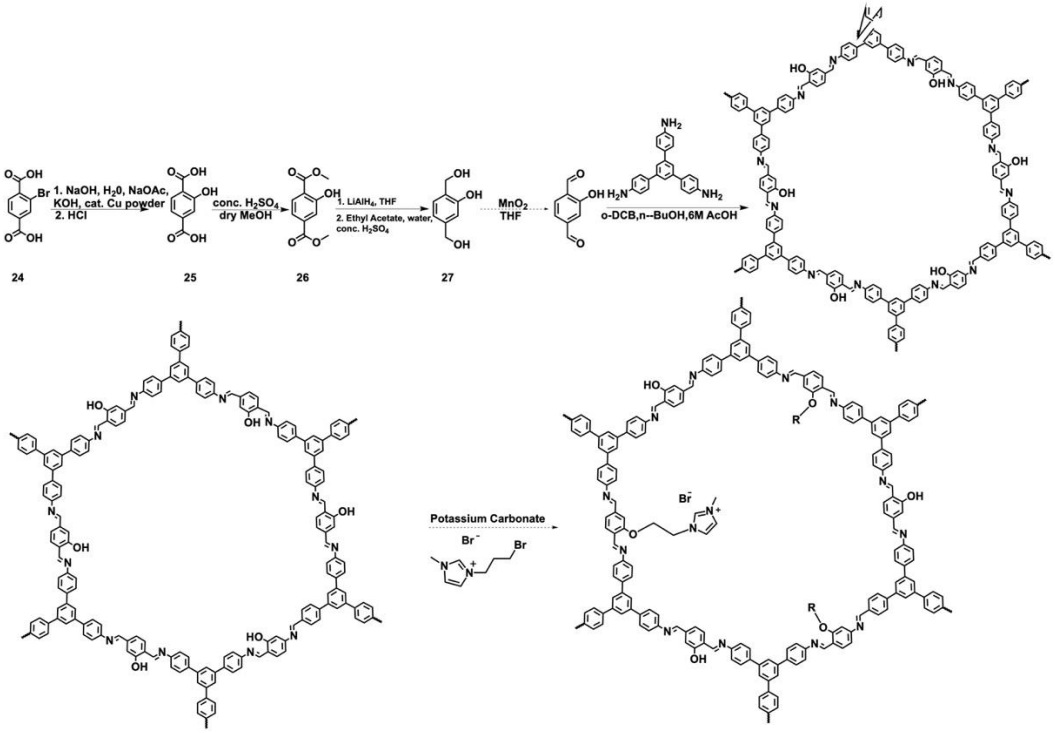

Scheme 3.1. Proposed scheme for synthesis of COF-HNU3.

The conversion of 2-bromoterephthalic acid (**24**) into 2-hydroxyterephthalic acid (**25**) proved more challenging than the literature supported, taking additional four days than the reported time and producing a lower yield. Eventually, a reasonably priced source of **25** was found, allowing us to skip this step of the synthesis process. From there, dual-esterification into dimethyl 2-hydroxyterephthalate (**26**) using methanol and sulfuric acid was near quantitative. However, the reaction reducing **26** into 2,5-bis(hydroxymethyl)phenol (**27**) using lithium aluminum hydride ($LiAlH_4$) proved difficult. This step was only done to successful completion one time, as confirmed *via* ^1H NMR spectroscopy. Literature reports state that the compound should be neutralized, then isolated via extraction. However, we always obtained it as an impure oil. Due to

simpler and cheaper reaction conditions, we decided to focus on the synthesis of COFs containing NHCs in the pore walls.

3.5 Framework Linkers containing NHCs.

Next, we focused on the work of the Cao research group. Specifically, we explored the synthesis of Im-COF1 (**28**) and its use of 4,7-bis(4-formylbenzyl)-1-methyl-1H-benzimidazole (BFMBIM) (**29**) which is commercially available. Their elegant use of dimethyl carbonate (DMC) to both alkylate the imidazole as well as form the carbene and protect it with CO_2 proved intriguing (Scheme 3.2).

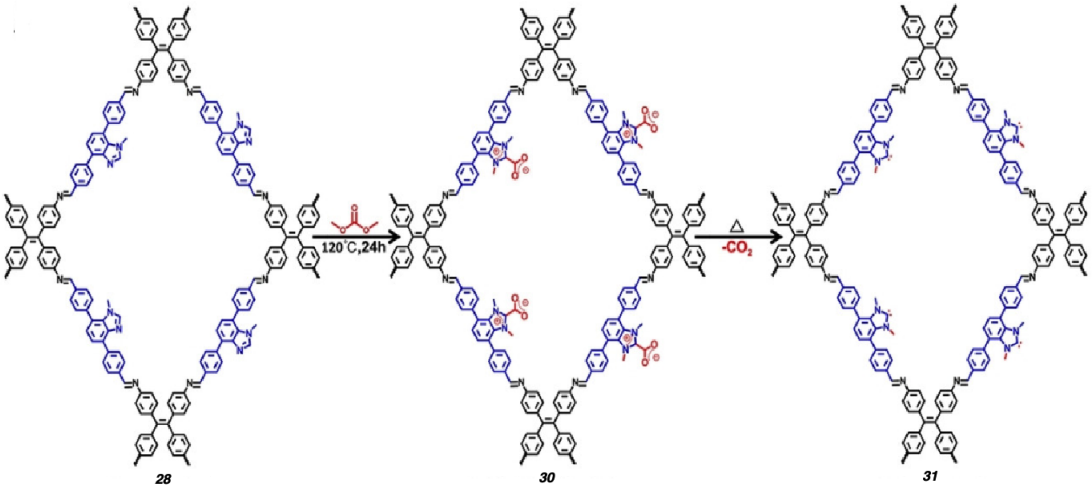

Scheme 3.2. Proposed scheme for synthesis of **28, 30,** and **31**. (Reprinted with permission from Figure 1 Copyright 2022 Wiley-VCH GmbH.)

We investigated DMC's compatibility with the parent, **29**, as reported in the literature. **29** was suspended in DMC and heated to 120 ^{o}C in a pressure tube equipped with a teflon cap. No visual change or change in the ^{1}H NMR spectra lead to investigation into other alkylating methods. We also found other mentions in the

literature of using DMC in a similar manner, but at temperatures as high as 170 °C,[33] and we still noticed no change (Figure 3.3).

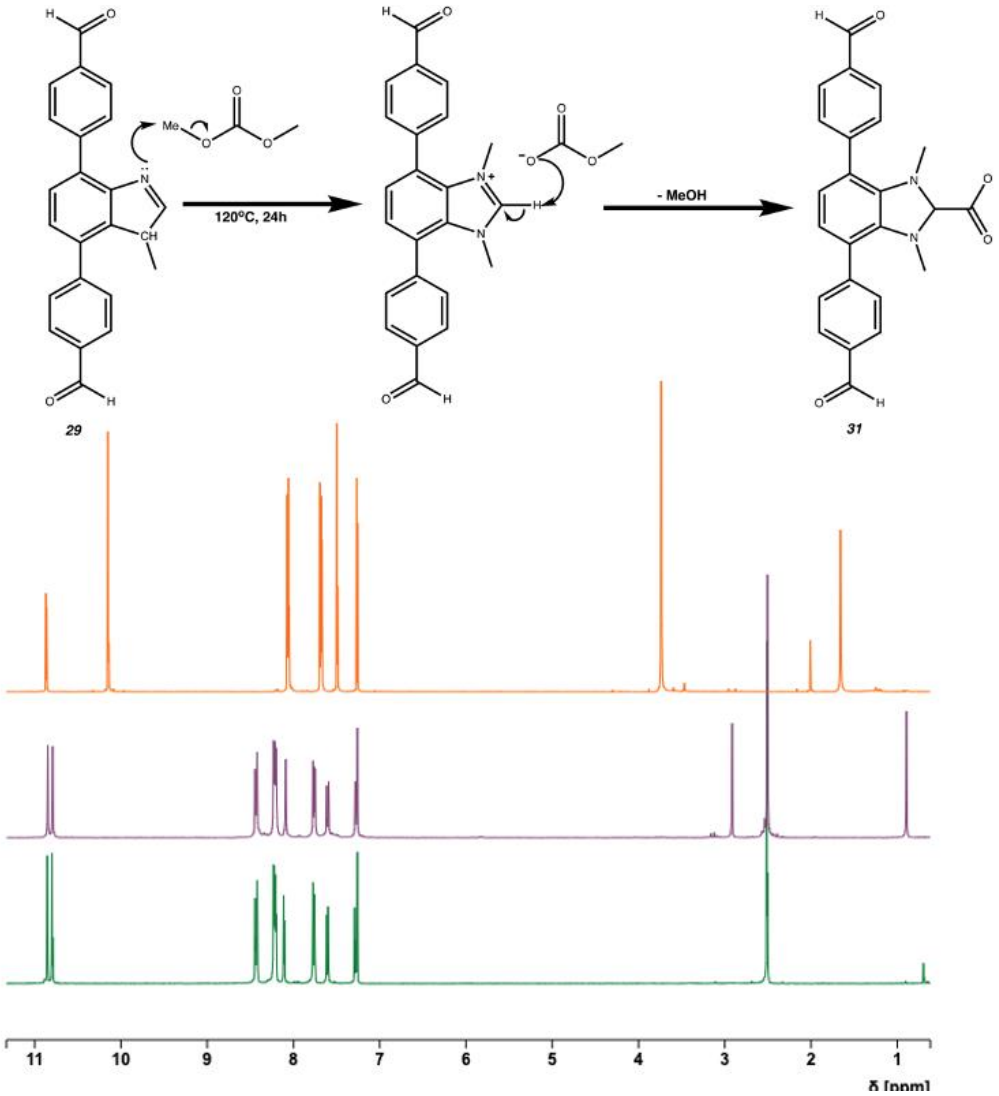

Figure 3.3. ^{1}H NMR Spectroscopy of **29** (green), after 26 hours @ 120°C (purple), and predicted product (orange) in $CDCl_3$.

We also moved away from 4,4′,4″,4‴-(ethene-1,1,2,2-tetrayl)-tetraaniline to the less flexible 1,3,5-Tris(4-aminophenyl)benzene (**32**) in hopes of obtaining a crystalline material (Scheme 3.3).[34]

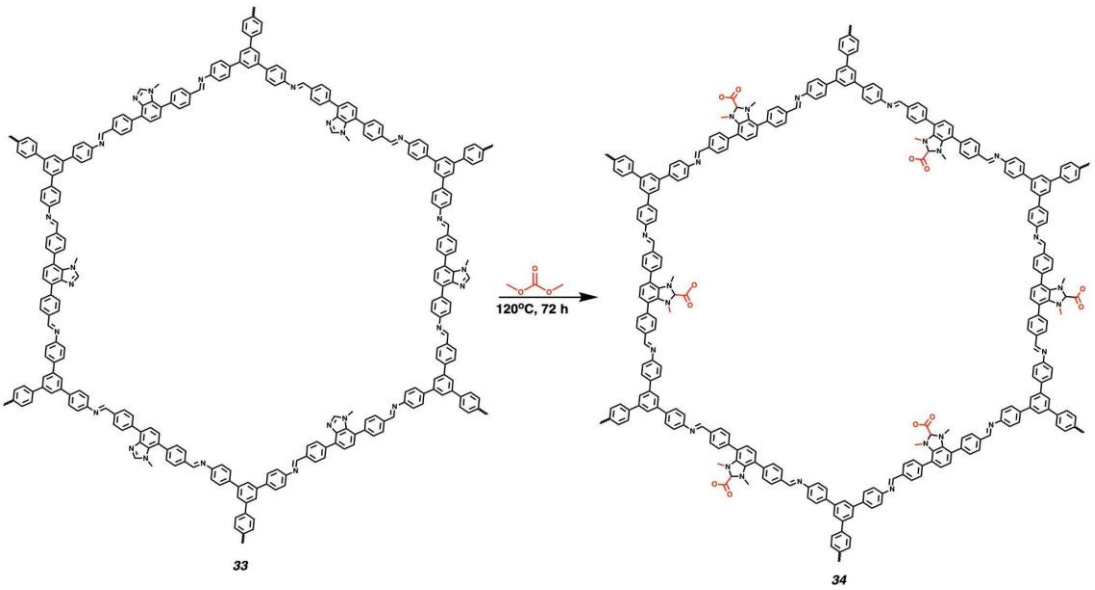

Scheme 3.3. Proposed scheme for synthesis of COFs **33** and **34**.

At first efforts to combine **32** and **29** produced an amorphous material, **33**. However, we later learned this was from pore collapse due to using the traditional vacuum activation method to remove solvents. Once we switched to the aforementioned gentle dying method, (Figure 3.4) we were able to achieve powder X-ray diffraction (PXRD) data confirming its crystallinity with the help from Dr. Akhilesh Tripathi at Rigaku Americas.

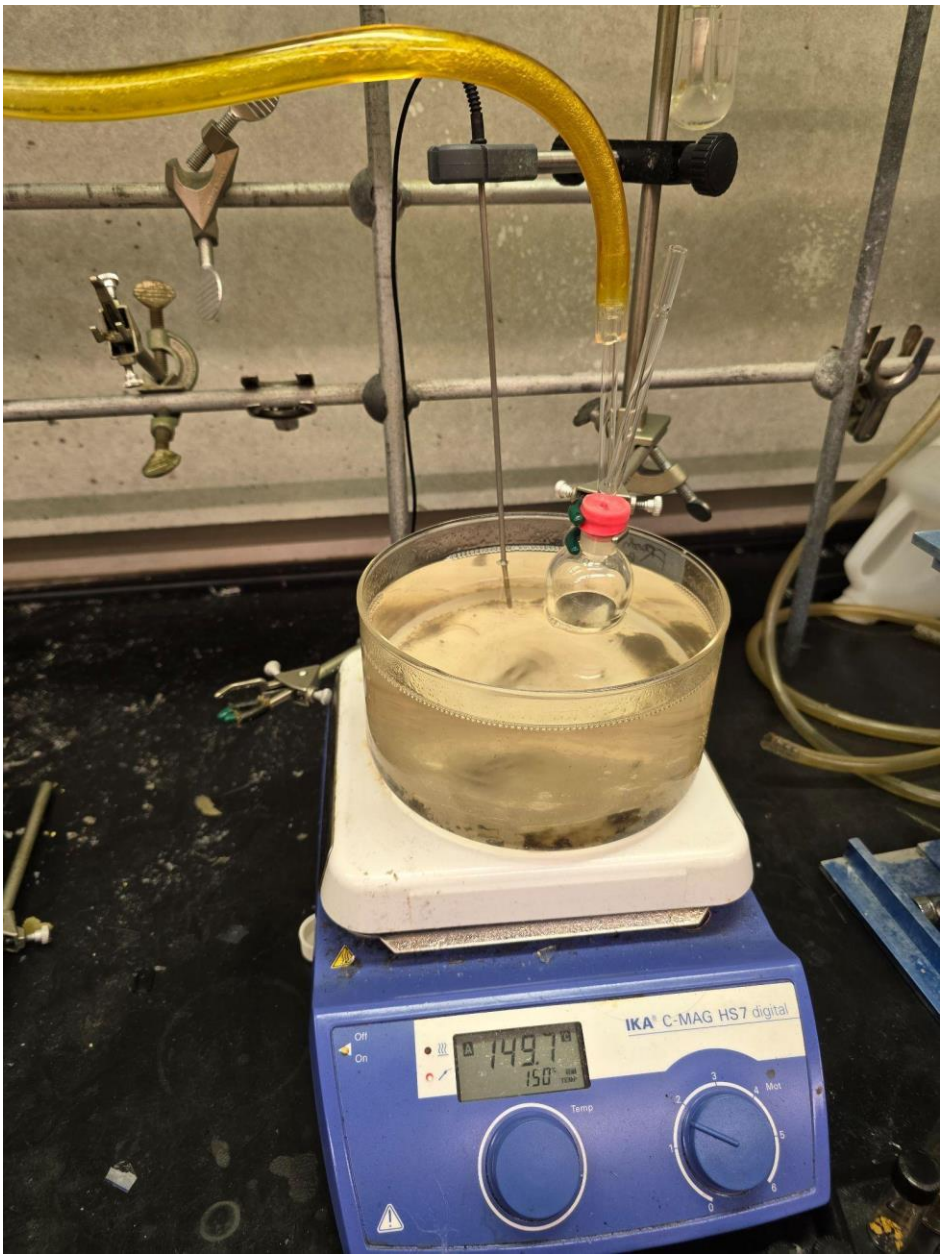

Figure 3.4. Gentle Nitrogen Drying apparatus; A round bottom was fitted with a rubber septum which had two pipettes piercing it. One of the pipettes was for off-gassing purposes, while the other was connected to a nitrogen tank via a Schlenk line. This round bottom was then placed in an oil heating bath @150 ºC for three hours.

We were also able to achieve scanning electron microscopy (SEM) spectra that matched the literature in appearance (Figure 3.5).

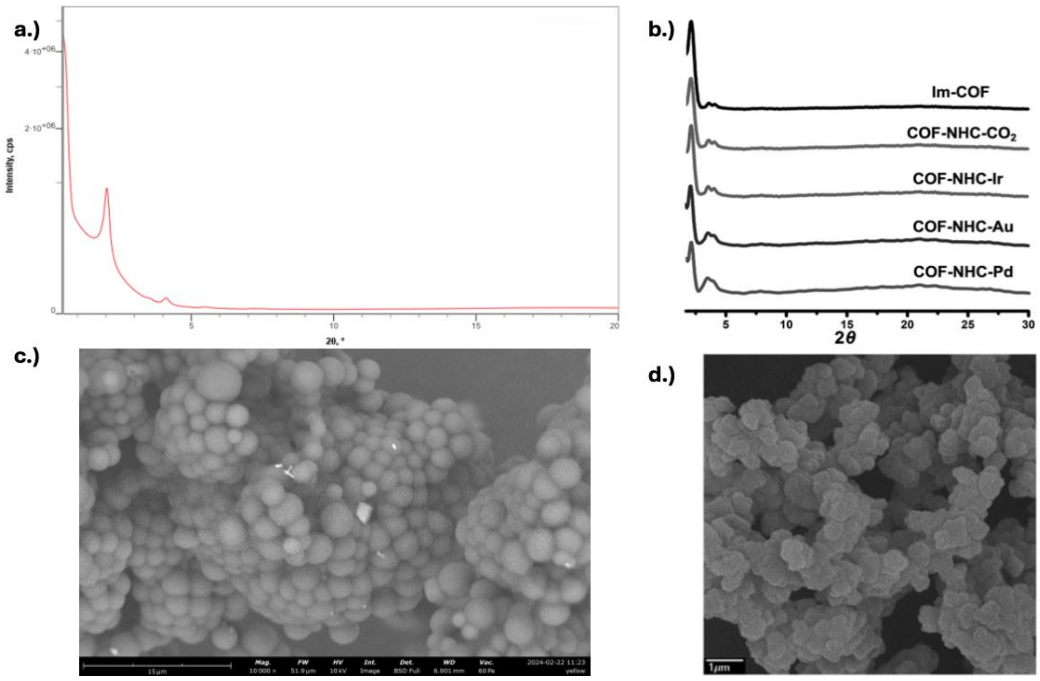

Figure 3.5. a.) PXRD Data of synthesized **33;** b.) PXRD Data reported in literature; c.) SEM spectra of synthesized **33**; d.) SEM spectra reported in literature.

With preparation of a crystalline framework, the next step was to alkylate the framework so that it can be converted into an NHC via deprotonation in the future (Scheme 3.4).

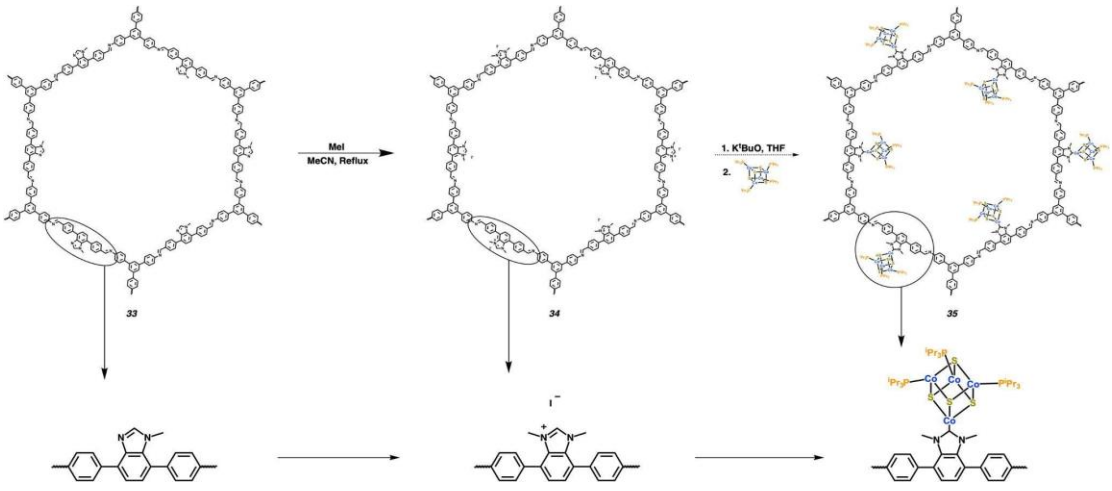

Scheme 3.4. Proposed Scheme for the formation of the NHC-COF (**34)** and the PSM of the COF with the Co_4S_4 cluster (**35**).

Retaining crystallinity post-alkylation proved troublesome for us. We propose that methyl iodide is reacting with the imine instead of the imidazole, or there is an issue with the iodine ion, disrupting the framework and ruining crystallinity. In an attempt to alkylate without crystalline disruption a variety of bromide alkylating agents, such as, butyl bromide, ethyl bromide, and butyl bromide were employed. (Figure 3.6). Butyl bromide showed no change in the ^{1}H NMR spectra. Ethyl bromide resulted in minor alkylation, 5%, but did not progress further after 1 week. Benzyl bromide resulted in complete alkylation. This is confirmed by the peak at 11.3 ppm integrating to 1:2 in relation to the 2 aldehyde peaks at 10.1 ppm, indicating it is the imidazolium proton. However, impurities remained present, indicating the need to investigate purification methods. Milder conditions, such as lower temperatures and lesser equivalents of the alkylating agents, were also employed, but these were not able to preserve crystallinity.

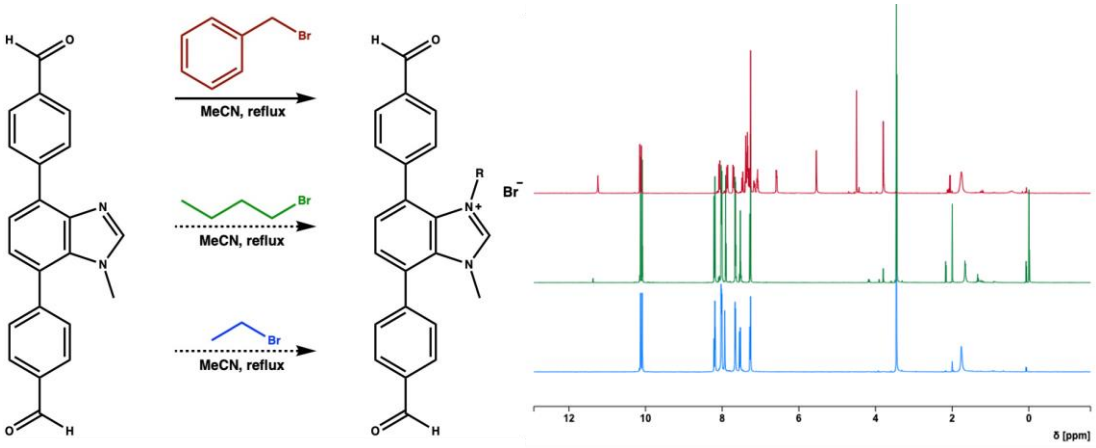

Figure 3.6. ^{1}H NMR spectra of **29** after butyl bromide (blue), ethyl bromide (green), and benzyl bromide (red).

Other milder approaches including use of the imidazolium salt instead of the imidazole for COF formation were also attempted, but crystalline material was never

obtained. This leads credence to the potential that the iodine ion was disrupting the framework in previous experiments. It has been shown that using modulators during framework formation is a way to improve crystallinity. Examples of this would be simpler molecule competes with the imine linking of the framework, allowing for error correction in the crystal lattice to occur (Figure 3.7).[35]

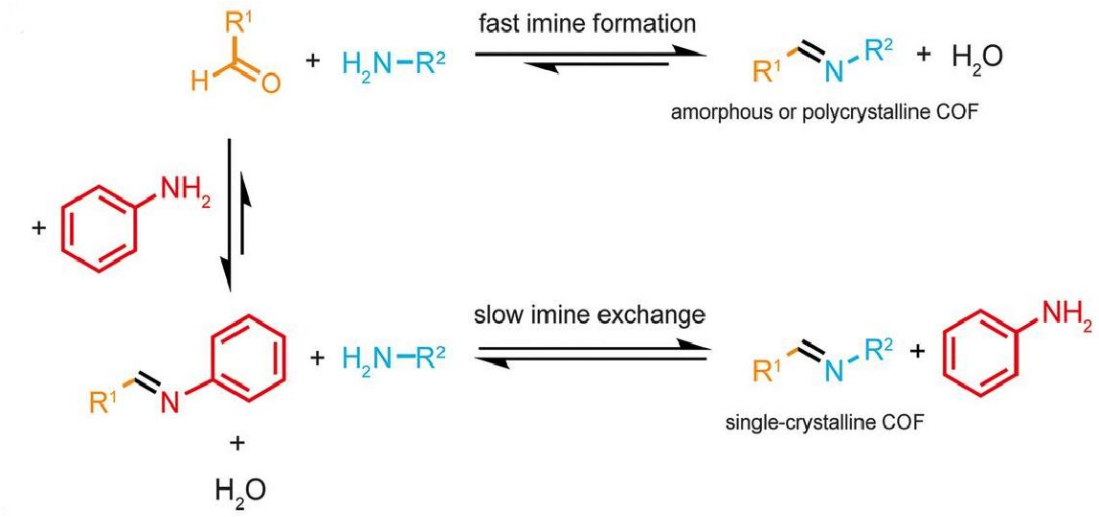

Figure 3.7. Proposed Scheme for the use of modulators in COF formation to improve crystallinity. (Reprinted (adapted) with permission from Fig. 1 Copyright 2018 The American Association for the Advancement of Science.)

Along with use of modulators, other reaction conditions may be modified to improve crystallinity such as using Lewis acid metal triflates, like scandium(III) triflate, to catalyze the transimination process (Scheme 3.5).[36]

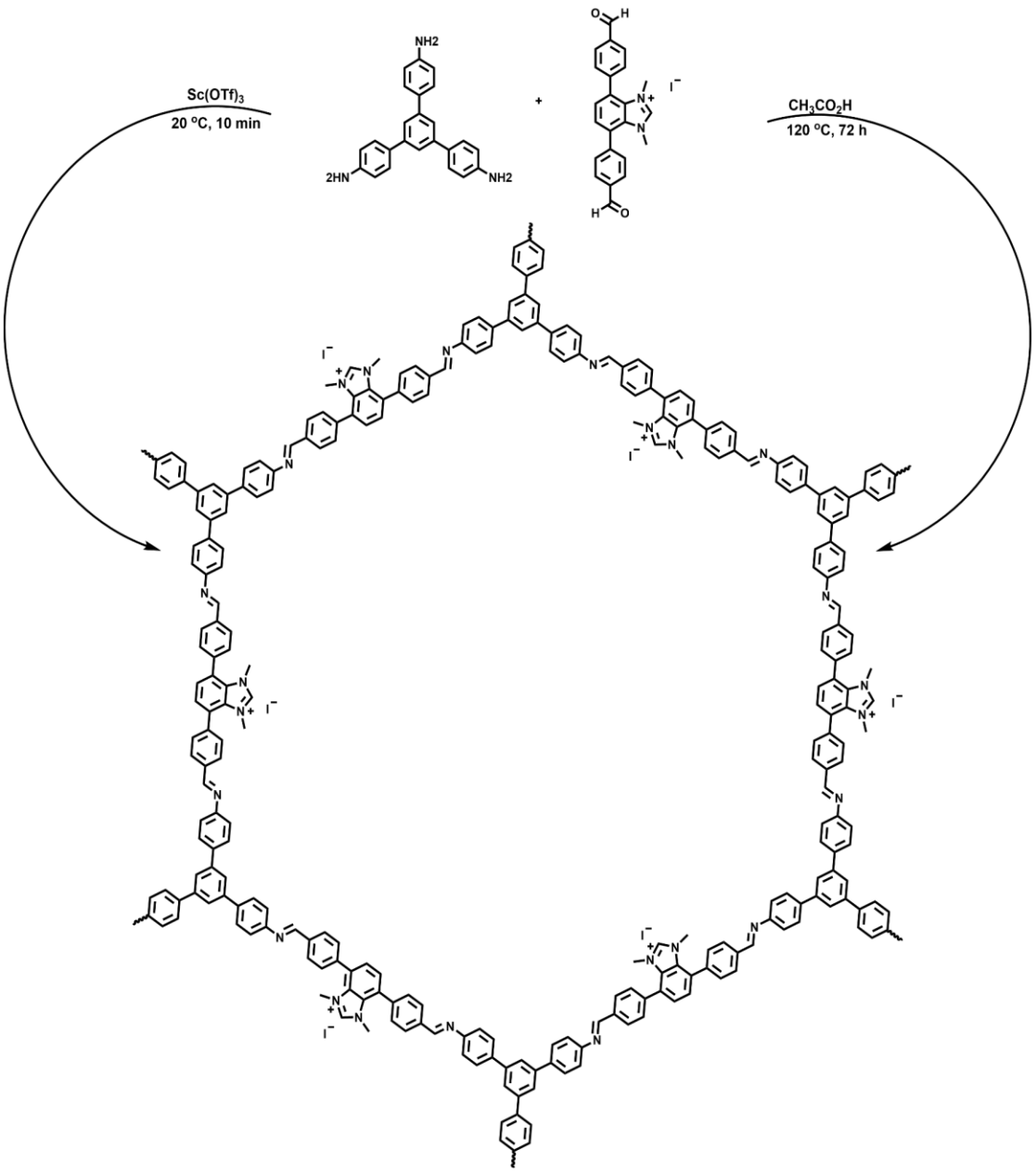

Scheme 3.5. Two pathways for the synthesis of **33**, the more traditional acetic acid method, and the proposed, scandium(III) triflate method.

We attempted to employ these techniques for our frameworks, but these too yielded amorphous solids, likely due to our continued usage of methyl iodide. We speculate that the increased size of the iodine ion, as compared to the bromine ion, is putting undo stress

onto the framework. This stress we theorize is disrupting the stacking of the COF, and as a result leading to an amorphous solid. Another pathway to crystalline NHC solids we have attempted was to recreate the PyTTA-BFBIM-iCOF (**36**) reported by Jiang's research group; however, we used an iodide salt instead of a bromine salt (Scheme 3.6). Ultimately this framework was also concluded to be an amorphous solid *via* PXRD analysis, further strengthening our thoughts that the iodine ion is in part responsible for disrupting framework crystallinity. The bromine imidazolium salt is known in the literature of its synthesis; however, methyl bromide is required. Due to the safety concerns of working with a toxic gas, the bromide salt was not synthesized.[37]

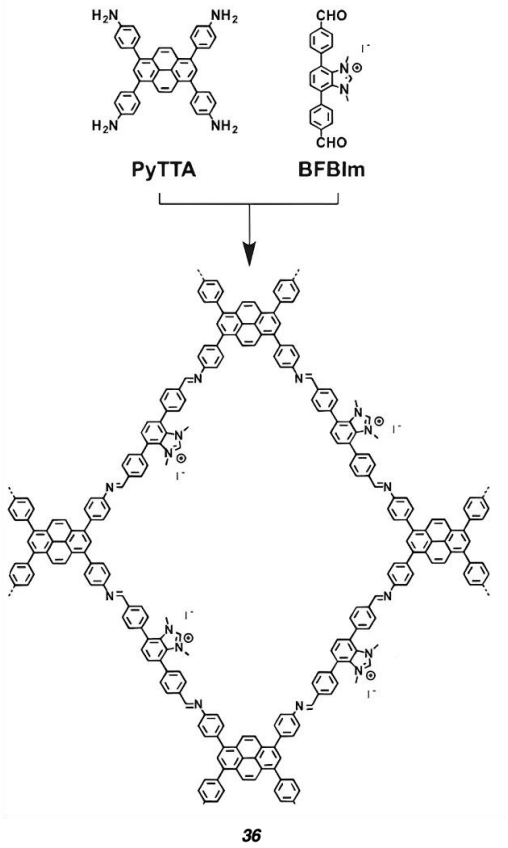

Scheme 3.6. Modified synthesis of **36.** (Reprinted (adapted) from Figure 1 Copyright 2017 Wiley-VCH Verlag GmbH & Co. KGaA, Weinheim.)

Our most recent endeavor has involved the transformation of the sensitive imine-COF into the more robust benzoxazole-COF (**38**) in efforts to retain crystallinity following alkylation (Scheme 3.7).[38]

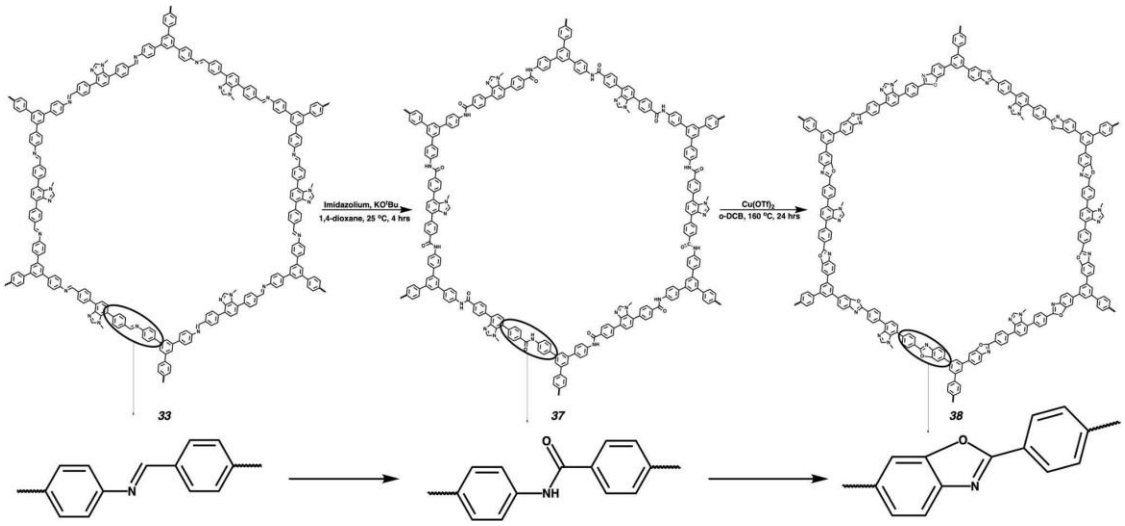

Scheme 3.7. Proposed scheme for the transformation of **33** into **38**.

Preliminary analysis of the infrared (IR) spectra notes the appearance and subsequent disappearance of a broad peak at 3300 ppm (Figure 3.8). This indicates the formation and dissolution of the amide-COF (AmCOF) (**37**) intermediate. Due to time constraints, PXRD analysis has not been run on the **38** yet.

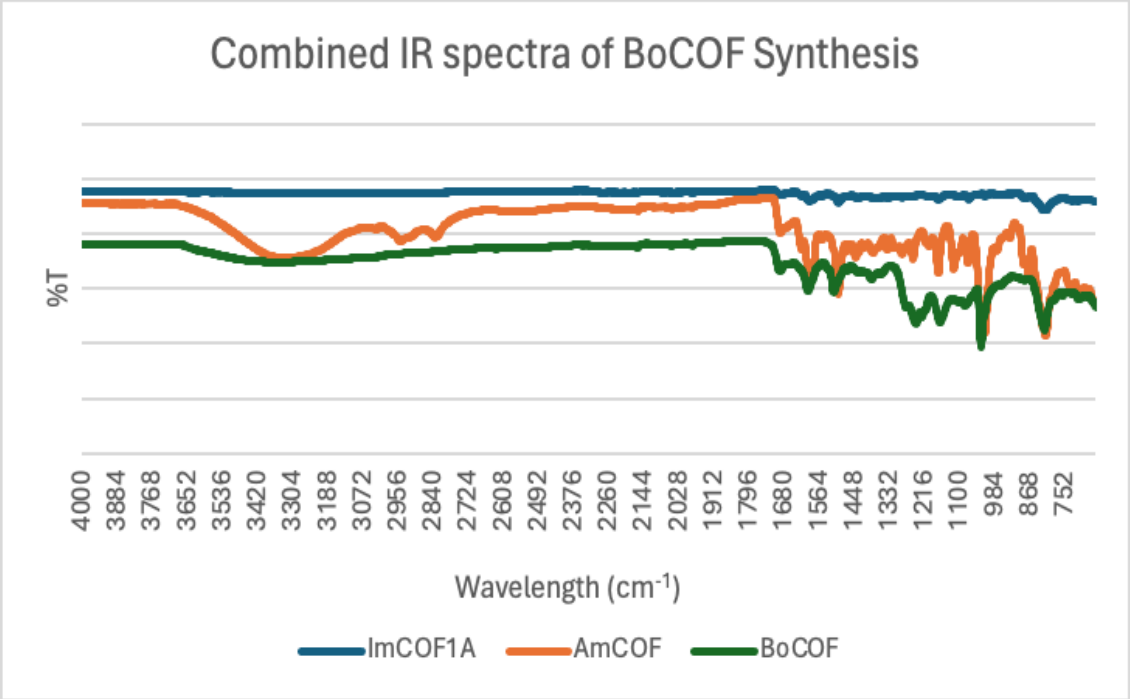

Figure 3.8. Combined IR spectra of **33** (blue), **37** (orange), and **38** (green).

3.6 Conclusion

Functionalized NHCs as a means to coordinate discrete Co_4S_4 clusters with known metal centers for the formation of MOFs remains a challenging task. This is due to the challenge of retaining enough nucleophilic strength of the carbene to fully displace phosphine ligands in the $Co_4S_4(^iPr_3P)_4$, as well as finding suitable crystallization methods. Issues also arise during purification, leading to challenges in characterization as well as framework synthesis. Efforts to functionalize other materials, such as COFs, with NHCs for use in ligation of the $Co_4S_4(^iPr_3P)_4$ cluster were also attempted. However, these also proved difficult due to the apparent sensitivities of the crystallinity of these materials when in the presence of the iodine counter ion, or alkylating agents present in the NHC's precursor's synthesis. Attempts to circumvent this through the use of milder alkylating conditions or modulating techniques were employed to minimal success. With the

reopening of the Argonne National Laboratory, and the use of their synchrotron for PXRD analysis, better screening should be possible in the future, allowing for a broader approach towards investigating potential framework materials. Efforts to overcome these obstacles would lead to materials which would provide novel ways to investigate these otherwise sensitive discrete clusters.

With imidazole-based COFs already being attainable, as seen in the synthesis of **33**, conversion into the desirable NHC-functionalized COFs remain only a few steps away. Further purification of **29** alkylated with benzyl bromide would allow for elimination of the troublesome iodine counter ion, and replace it with the smaller, less disruptive bromide ion. Access to the bromide imidazolium should allow the synthesis of a crystalline version of **36**. Continued characterization of the more recent **38** also proves promising due to the increased stability to the framework it allows. With these new approaches, efforts to form a crystalline imidazolium and NHC-functionalized COFs should prove more successful.

3.7 Future work

COF synthesis methods provide many conditions which need to be fine-tuned to ensure crystallinity of this class of materials. Further efforts to distinguish these conditions would enable the use of these frameworks for use as scaffolds for a multitude of discrete clusters. Most notably, if NHC-functionalized COFs can be synthesized they allow another avenue to investigate the properties of the elusive $Fe_4S_4^0$ cluster. Due to the immaculate surface area and porosity of these framework materials they would also allow the development of new materials for gas storage or electrochemical applications. Future efforts should also be made to investigate the crystallinity of **38** *via* PXRD analysis, as

well as further confirmation of formation *via* solid state ^{13}C NMR. Should these efforts prove successful, alkylating using methyl iodide or benzyl bromide should be investigated, to determine their effects on its crystallinity in efforts to achieve NHC-functionalized COFs.

3.8 Experimental

Synthesis of 1H-Benzimidazolium, 5-bromo-1,3-bis(1-methylethyl)-, iodide **19**. Prepared according to published literature.[26]

18 (1 g, 5.08 mmol), potassium carbonate (0.84 g, 6.1 mmol), and 2-iodopropane (2.9 mL, 10.2 mmol) were combined in a Schlenk flask (50 mL) along with acetonitrile (50 mL). The solution was then heated at reflux overnight. After cooling to room temperature 2-iodopropane (11.9 mL, 146 mmol) was added and the suspension was refluxed for an additional 72 hours under N_2. Volatiles were then removed, and it was filtered through Celite using DCM. DCM was removed via rotary evaporation and then the product was recrystallized out of methanol and diethyl ether resulting in a yellow solid (1 g, 48%). ^1H NMR shifts matched those reported.

Synthesis of 5-bromo-1,3-bis(1-methylethyl)-NHC-benzimidazole **20.** Prepared according to published literature.[25]

19 (0.15 g, 0.37 mmol) was suspended in THF (9 mL). Potassium tert-butoxide (0.43 mg, 0.39 mmol) was added and stirred for 75 mins, and then the resulting suspension was filtered using a syringe filter. 100% yield was assumed. ^1H NMR (500 MHz, benzene-*d*6) δ = 7.09 (s, 1H), 6.59 (s, 1H), 6.58 (s, 1H), 4.19 (sept, 1H), 4.01 (sept, 1H), 1.36 (dd, 12).

Synthesis of $Co_4S_4(^iPr_2NHCBr)_4$ **21.**

$Co_4S_4(^iPr_3P)_4$ (25.5 mg, 0.025 mmol) dissolved in THF (5 mL) was combined with **20** (41.5 mg, 0.10 mmol) in a tube sealed with a teflon screw cap and heated at 70 ^oC 32 h. ^1H NMR (500 MHz, benzene-*d*6) was conducted, but proved too convoluted to decipher due to impurities.

Synthesis of $Co_4S_4(^iPr_2NHCCOOH)$ **22.** Adapted from published literature.[39]

21 (50 mg, 0.0336 mmol) was dissolved in THF (6 mL) in a Schlenk flask. The solution was cooled to -78 ^oC, upon which 2.7M *n*-Butyllithium in toluene (0.05mL, 0.13 mmol) was added dropwise over the course of 2 minutes under constant stirring. CO_2(g) was bubbled into the reaction for 30 mins. Solvent was then removed *via* vacuo, upon which the precipitate transferred into a N_2 filled glovebox, upon which it was triturated with diethyl ether and THF. The solid was then suspended in THF (5 mL) upon which it was acidified with 2M HCl in diethyl ether (0.4 mL). Residual solvents were removed *via* vacuo and then washed with DCM leaving a dark green solid. ^1H NMR (500 MHz, benzene-*d*6) was conducted, but proved too convoluted to decipher due to impurities.

Synthesis of Ethyl benzimidazole-6-carboxylate **2.** Prepared according to published literature.[23]

1 (5g, 31 mmol) was dissolved in ethanol (100 mL) and had concentrated sulfuric acid (4 mL) added slowly then refluxed for 1 hr. After 1 hr the heat was reduced to 60 ^0C overnight. Volatiles were removed and then the product was extracted with ethyl acetate and a saturated sodium carbonate solution; the organic layers were combined before washed with brine, dried with sodium sulfate. The solvents were then removed via rotary

evaporation to reveal a pale pink solid (3.2g, 54%). ^{1}H NMR shifts matched those reported.

Synthesis of Ethyl-5/6-(1-isopropylbenzimidazole) carboxylate **7.** Prepared according to published literature.[23]

2 (1 g, 5.3 mmol) and cesium carbonate (2.8g, 8.6 mmol) was suspended in acetonitrile (40 mL). To the stirred suspension was added 2-bromopropane (1.4 mL, 15 mmol) and then refluxed overnight. The suspension was cooled to room temperature before volatiles were removed and then filtered through Celite using DCM. column chromatography was then performed using DCM/Methanol (95:5) with a rf of 0.64 resulting in a yellow oil (0.46 g, 37%). ^{1}H NMR shifts matched those reported.

Synthesis of Ethyl-5-(1,3-diethylbenzimidazole) carboxylate bromide **3**. Adapted from published literature.[25]

2 (670 mg, 3.5 mmol) and sodium bicarbonate (607 mg, 7.2 mmol) were dissolved in acetonitrile (5 mL); the solution was then refluxed for 1 hr. The reaction was then cooled to room temperature, and bromoethane (1.6 mL, 21 mmol) was added and the solution was refluxed overnight. The suspension was filtered, and solvents were removed via rotary evaporation to give a pale brown solid (0.97g, 84%). ^{11}H NMR (500 MHz, chloroform - *d*3) δ = 11.7 (s, 1H), 8.41 (s, 1H), 8.35 (dd, 1H), 7.77 (dd 1H), 4.73 (q, 4H), 4.49 (q, 2H), 1.78 (t, 6H), 1.45 (t, 3H).

Synthesis of Ethyl 1,3-diethylbenzimidazole-6-carboxylate NHC **4.**

3 (73 mg, 0.22 mmol) was suspended in THF (5 mL). Potassium tert-butoxide (25 mg, 0.22 mmol) was added and the reaction was stirred while heated to 55 ^{o}C in a 1 dram vial overnight. Once cooled to ambient temperature the suspension was filtered through a syringe filter. ^{1}H NMR (500 MHz, benzene-*d*6) was conducted, but proved too convoluted to decipher due to impurities.

Synthesis of Ethyl-5-(1,3-dibenzylbenzimidazole) carboxylate bromide **12**. Prepared according to published literature.[24]

2 (0.86 g, 4.5 mmol) was dissolved in acetonitrile (27 mL). Sodium hydroxide (0.18 g, 4,5 mmol) was added to the solution and stirred for 30 mins. Benzyl bromide (0.54 mL, 4.5 mmol) was added to the reaction and the solution was refluxed overnight. After cooling to ambient temperature volatiles were removed and the resultant solid was dissolved in THF, filtered then volatiles were removed again. The reluctant oil was dissolved in toluene (80 mL) and benzyl bromide (0.54 mL, 4.5mmol) was added to the stirring solution. The reaction was refluxed overnight, after which product was recrystallized with diethyl ether (80% yield). ^{1}H NMR shifts matched those reported.

Synthesis of Ethyl-5-(1,3-dibenzylbenzimidazole) carboxylic acid chloride **13**. Prepared according to published literature.[24]

12 (0.45 g, 1.0 mmol) in 6 M aqueous HCl (15 mL) was refluxed for 36 h. The precipitate was collected via filtration and rinsed with deionized water and acetone sequentially (91% yield). ^{1}H NMR shifts matched those reported.

Synthesis of Ethyl-5-(1,3-dibenzylbenzimidazole) carboxylate **15.**

13 (25 mg, 0.05 mmol) in THF (5mL) was added KO^{t}Bu (5.6 mg, 0.05 mmol) and stirred at 60 ^{o}C overnight. Precipitate was collected *via* centrifugation and washed with THF. Product was confirmed *via* ^{1}H NMR spectroscopy (100% yield). ^{1}H NMR (500 MHz, DMSO-*d*6) δ = 10.07 (s, 1H), 8.41 (s, 1H), 8.15 (d, 1H), 7.96 (d, 1H), 7.4-7.5 (m, 10H), 5.86 (s, 2H), 5.79 (s, 2H).

Synthesis of 2-Hydroxyterephthalic acid **25**. Prepared according to published literature.[40]

24 was mixed with 2 equivalents of NaOH in water until dissolved. Once dissolved 2.5 equivalents of NaOAc was added along with a catalytic amount of Cu powder; this suspension was then heated to reflux. According to the literature it should have only needed to reflux for 3 days. However, the time taken was 7 days on average for me, otherwise some starting material would remain. ^{1}H NMR shifts matched those reported.

Synthesis of Dimethyl 2-Hydroxyterephthalate **26**. Prepared according to published literature.[41]

25 (0.55 g, 3.02 mmol) was dissolved in 58 mL of methanol. Sulfuric acid (4 mL) was added dropwise and reflux overnight. The solution was cooled to room temperature upon which it was neutralized with a 150 mL sodium bicarbonate solution and then extracted with DCM (6x25 ml). The organic layer was isolated and washed with brine before drying with sodium sulfate. Sodium sulfate was then removed, and the solvent was evaporated to produce a cream-colored powder (0.3624 g, 57%). ^{1}H NMR shifts matched those reported.

Synthesis of 2,5-Bis(hydroxymethyl)phenol **27**. Prepared according to published literature.[41]

26 (1.5 g, 7.14 mmol) was placed inside a Schlenk flask and dissolved in 60 mL of anhydrous THF while under nitrogen. Lithium aluminum hydride (4x 300 mg, 32.11mmol) was added slowly while stirring; once added the reaction was set to reflux for 2.5 days. The suspension was coolest to room temperature and then placed in an ice bath. Water and ethyl acetate were added to neutralize leftover lithium aluminum hydride. Sulfuric acid was added, resulting in a red solution. The product was extracted with ethyl acetate, and solvent was evaporated to give a yellow oil; addition of benzene caused the product to precipitate out in the form of a white solid. ^{1}H NMR shifts matched those reported.

Synthesis of Im-COF-1 **28**. Prepared according to published literature.[30]

29 (54.5 mg, 0.16mmol) and 4,4′,4″,4‴-(ethene-1,1,2,2-tetrayl)-tetraaniline (30.2 mg, 0.08 mmol) were placed in in a 10 mL sealable pressure tube. An o-DCB/*n*-BuOH/6M acetic acid mixture (2 mL/2 mL/0.2 mL) was added, promptly followed by 15 minutes of sonication. The tube then went through three degas cycles before being sealed and placed in an oven at 120 ^{o}C for three days. The tube was cooled to RT before opened, and the solid was collected by filtration and rinsed with THF until the filtrate ran clear. The solid was then suspended in MeOH (5 mL) for a total of 2 hours, replenishing the MeOH after an hour; the solvent was then switched for DCM and then hexane, following the same procedure as with MeOH. The solid was then heated to 150 ^{o}C under N_2 for 3 hours.

Synthesis of COF1A **33**. Adapted from published literature.[34]

29 (40 mg, 0.118 mmol) and **32** (28 mg, 0.08 mmol) were placed in a 10 mL sealable pressure tube. A 1,4-dioxane/mesitylene/6M acetic acid mixture (2 mL/2 mL/0.2 mL) was added, promptly followed by 15 minutes of sonication. The tube was then placed in an oven at 120 ^{o}C for three days. The tube was cooled to RT before opened, and the solid was collected by filtration and rinsed with THF until the filtrate ran clear. The solid was then suspended in MeOH (5 mL) for a total of 2 hours, replenishing the MeOH after an hour; the solvent was then switched for DCM and then hexane, following the same procedure as with MeOH. The solid was then heated to 150 ^{o}C under N_2 for 3 hours.

Synthesis of ICOF **34**. Adapted from published literature.[31]

5,6-bis(4-formylbenzyl)-1,3-dimethyl-benzimidazolium iodide (57 mg, 0.118 mmol) and **32** (28 mg, 0.08 mmol) were placed in in a 10 mL sealable pressure tube. An o-DCB/*n*-BuOH/6M acetic acid mixture (2 mL/2 mL/0.2 mL) was added, promptly followed by 15 minutes of sonication. The tube was then placed in an oven at 120 ^{o}C for three days. The tube was cooled to RT before opened. The solid was collected by filtration and rinsed with THF until the filtrate ran clear. The solid was then suspended in MeOH (5 mL) for a total of 2 hours, replenishing the MeOH after an hour; the solvent was then switched for DCM and then hexane, following the same procedure as with MeOH. The solid was then heated to 150 ^{o}C under N_2 for 3 hours.

Synthesis of PyTTA COF **36**. Adapted from published literature.[37]

4,4′,4″,4‴-(pyrene-1,3,6,8-tetrayl)tetraaniline (22.6 mg, 0.02mmol) and 5,6-bis(4-formylbenzyl)-1,3-dimethyl-benzimidazolium iodide (38.6 mg, 0.04 mmol) were place in a sealable pressure tube along with a o-DCB/*n*-BuOH (1 mL/1 mL) mixture. The tube was then sonicated for 15 minutes to ensure the suspension was homogenous before doing three freeze-pump-thaw cycles to degas the reaction. The tube was then sealed and placed in an oven at 120 ^{o}C for three days. Once room temperature the tube was opened, and the solid was rinsed with THF until it ran clear. The solid was then suspended in MeOH (5 mL) for a total of 2 hours, replenishing the MeOH after an hour; the solvent was then switched for DCM and then hexane, following the same procedure as with MeOH. The solid was then heated to 150 ^{o}C under N_2 for 3 hours.

Synthesis of MeLZU-79 COF. Adapted from published literature.[35]

29 (8.8 mg, 0.026 mmol) was suspended in THF/MeCN (0.25 mL/0.25 mL) in a 1 dram vial. Trifluoroethylamine (60 μL) was added along with trifluoroacetic acid (0.1 mL). Tetrakis(4-aminophenyl)methane (5 mg, 0.013 mmol) was dissolved in THF/MecN (0.25 mL/0.25 mL) in a separate vial. The dissolved solution of Tetrakis(4-aminophenyl)methane was added to the 1 dram vial of 4,4'-(1-Methyl-1H-benzimidazole-4,7-diyl)bis[benzaldehyde]. The solution was passed through a filter into another 1 dram vial and let sit at room temperature for 2.5 days to reveal a pale yellow precipitate.

Synthesis of Scandium Triflate COF1A. Adapted from published literature.[36]

29 (51 mg, 0.15 mmol) and ***32*** (36 mg, 0.1 mmol) were placed in a 1 dram vial along with chloroform (4mL). Scandium(III) triflate (3 mg, 0.006 mmol) was added and

the vial was sonicated for 10 minutes. After sonication the vial was left to sit for 24 hrs at room temperature, at which point a yellow precipitate had formed.

Synthesis of Scandium Triflate ICOF. Adapted from published literature.[36]

5,6-bis(4-formylbenzyl)-1,3-dimethyl-benzimidazolium iodide (72 mg, 0.15 mmol) and **32** (36 mg, 0.1 mmol) were placed in a 1 dram vial along with chloroform (4mL). Scandium(III) triflate (3 mg, 0.006 mmol) was added and the vial was sonicated for 10 minutes. After sonication the vial was left to sit for 24 hrs at room temperature, at which point a yellow precipitate had formed.

Synthesis of Triethyl Orthoformate COF. Adapted from published literature.[42]

29 (50 mg, 0.15 mmol) and ammonium tetrafluoroborate (19 mg, 0.18 mmol) were suspended in triethyl orthoformate (1 mL) and heated to 125 ^{o}C under N_2 for 24 hrs. The solution was cooled to room temperature and volatiles were evacuated via rotary evaporation. The resulting oil was dissolved methanol/ ethyl acetate (1:1) and filtered through basic alumina. Solvents were removed via rotary evaporation again, resulting in a red powder.

Synthesis of AmCOF **37**. Adapted from published literature.[38]

33 (83.5 mg, calculated 0.1mmol) was added to 1,3-diisopropylbenzimidazolium-6-bromide hexafluorophosphate (50.3 mg, 0.12mmol) dissolved in 1,4-dioxane (4 mL). KO^{t}Bu (22.4, 0.2mmol) was added. The reaction was stirred at room temperature for 4 hours. Upon completion the solid was collected by filtration and washed sequentially with methanol and water.

Synthesis of Benzoxazole-COF **38**. Adapted from published literature.[38]

37 (112 mg, calculated 0.2 mmol) was added copper(II) triflate (72 mg, 0.2 mmol) in o-dichlorobenzene (2 mL) and the reaction was refluxed overnight. Upon completion, the solid was collected by filtration and washed with tetrahydrofuran, methanol, and hexane.

REFERENCES

1) Tanifuji, K.; Ohki, Y. *Chem. Rev.* **2020,** *120,* 5194-5251.
2) Bazylinski, D. A. *Chem. Geol.* **1996**, *132* (1-4), 191–198.
3) Wächtershäuser, G. *Prog. Biophys. Mol. Biol.* **1992**, *58* (2), 85–201.
4) Wächtershäuser, G. *Philos. Trans. R. Soc., B* **2006,** *1474,* 1787-1808.
5) Lee, S. C.; Lo, W.; Holm, R. H. *Chem Rev.* **2014,** *114,* 3579-3600.
6) Watt, G. D.; Reddy, K. R. N. *J. Inorg. Biochem.* **1994**, *53* (4), 281–294
7) Deng L.; Holm, R. H. *J. Am. Chem. Soc*. **2008**, *130*, 30, 9878–9886.
8) Deng, L.; Bill, E.; Wieghardt, K.; Holm, R. H. *J. Am. Chem. Soc.* **2009**, *131* (31), 11213–11221.
9) Shim, Y.; Yuhas, B. D.; Dyar, S. M.; Smeigh, A. L.; Douvalis, A. P.; Wasielewski, M. R.; Kanatzidis, M. G. *J. Am. Chem. Soc.* **2013**, *135* (6), 2330–2337.
10) Horwitz, N. E.; Xie, J.; Filatov, A. S.; Papoular, R. J.; Shepard, W. E.; Zee, D. Z.; Grahn, M. P.; Gilder, C.; Anderson, J. S. *J. Am. Chem. Soc.* **2019**, *141*, 9, 3940–3951.
11) Batten, S. R.; Champness, N. R. Chen, X.-M.; Garcia-Martinez, J.; Kitagawa, S.; Öhrström, L.; O'Keeffe, M.; Suh, M. P.; Reedijk, J. *Cryst. Eng. Comm.* **2012**, *14* (9), 3001.
12) Kalmutzki, M. J.; Hanikel, N.; Yaghi, O. M. *Sci. Adv.* **2018**, *4* (10).
13) Diercks, C. S.; Yaghi, O. M.. *Sci.* **2017**, *355* (6328).
14) Ma, S.; Zhou, H.-C. *Chem. Commun.* **2010**, *46* (1), 44–53.
15) Yap, M. H.; Fow, K. L.; Chen, G. Z. *Green Energy Environ.* **2017**, *2* (3), 218–245.

16) Taylor-Pashow, K. M. L.; Della Rocca, J.; Xie, Z.; Tran, S.; Lin, W. J*J. Am. Chem. Soc.* **2009**, *131* (40), 14261–14263.

17) Schnabel, J.; Ettlinger, R.; Bunzen, H. *ChemNanoMat* **2020**, *6* (8), 1229–1236.

18) Yusuf, V.,F.; Malek, N.,I.; Kailasa, S.K. *ACS Omega* **2022**, 7(49),44507-44531.

19) Salcedo-Abraira, P.; Biglione, C.; Vilela, F.; Erik Svensson Grape; Ureña, N.; Salles, F.; María Teresa Pérez-Prior; Willhammar, T.; Philippe Trens; Várez, A.; A. Ken Inge; Horcajada, P. *Chem. Mater.* **2023**, *35* (11), 4329–4337.

20) Freeman, M. B.; Edokobi, O. D.; Gillen, J. H.; Kocherga, M.; Dipple, K. M.; Jones, D. S.; Paley, D. W.; Wang, L.; Bejger, C. M. *Chem. - Eur. J.* **2020**, *26* (55), 12523–12527.

21) Gillen, J. H.; Moore, C. A.; Vuong, M.; Shajahan, J.; Anstey, M. R.; Alston, J. R.; Bejger, C. M. *Chem. Commun.* **2022**, *58*, 4885 - 4888.

22) Li, M.; Li, D.; O'Keeffe, M.; Yaghi, O. *Chem. Rev.* **2014**, *114*, 2, 1343–1370.

23) Man, R. W. Y.; Li, C.-H.; MacLean, M. W. A.; Zenkina, O. V.; Zamora, M. T.; Saunders, L. N.; Rousina-Webb, A.; Nambo, M.; Crudden, C. M. *J. Am. Chem. Soc.* **2018**, *140* (5), 1576–1579.

24) Chang, L.-M.; An, Y.-Y.; Li, Q.-H.; Gu, Z.-G.; Han, Y.-F.; Zhang, J. *ACS Appl. Mater. Interfaces* **2020**, *12* (34), 38357–38364.

25) Joyce; Tennyson, A. G.; Kamplain, J. W.; Lynch, V. M.; Bielawski, C. W. *Eur. J. Inorg. Chem.* **2009**, *2009* (13), 1729–1738.

26) Sun, N.; Zhang, S.; Simon, F.; Anja Maria Steiner; Schubert, J.; Du, Y.; Qiao, Z.; Fery, A.; Lissel, F. *Angew. Chem., Int. Ed. Engl.* **2020**, *60* (8), 3912–3917.

27) Streich, D.; Yeni Astuti; Orlandi, M.; Schwartz, L.; Reiner Lomoth; Hammarström, L.; Ott, S. *Chem. - Eur. J.* **2009**, *16* (1), 60–63.

28) Pullen, S.; Fei, H.; Orthaber, A.; Cohen, S. M.; Ott, S. *J. Am. Chem. Soc.* 2013, 135, 45, 16997–17003.

29) Qiu, J.; Zhang, X.; Li, Z.; Wang, J.; Shi, Y.-L. *ChemSusChem* **2019**, *12* (11), 2421–2427.

30) He, C.; Si, D.; Huang, Y.; Cao, R. *Angew. Chem., Int. Ed. Engl.* **2022**, *61* (40).

31) Wu, Q.; Si, D.; Wu, Q.; Dong, Y.; Cao, R.; Huang, Y. *Angew. Chem., Int. Ed. Engl.* **2022**, *62* (7).

32) Feriante, C. H.; Jhulki, S.; Evans, A. M.; Dasari, R. R.; Slicker, K.; Dichtel, W. R.; Marder, S. R. *Adv. Mater.* **2019**, *32* (2), 1905776.

33) Maton, C.; Van Hecke, K.; Stevens, C. V. *New J. Chem.* **2015**, *39* (1), 461–468.

34) Rong, C.; Yuanbiao, H.; Chang, H. Preparation method and application of metal N-heterocyclic carbene functionalized covalent organic framework material CN 116082589A

35) Ma, T.; Kapustin, E. A.; Yin, S. X.; Liang, L.; Zhou, Z.; Niu, J.; Li, L.-H.; Wang, Y.; Su, J.; Li, J.; Wang, X.; Wang, W. D.; Wang, W.; Sun, J.; Yaghi, O. M. *Sci.* **2018**, *361* (6397), 48–52.

36) Matsumoto, M.; Dasari, R. R.; Ji, W.; Feriante, C. H.; Parker, T. C.; Marder, S. R.; Dichtel, W. R. *J. Am. Chem. Soc.* **2017**, *139* (14), 4999–5002.

37) Huang, N.; Wang, P.; Addicoat, M.; Heine, T.; Jiang, D. *Angew. Chem., Int. Ed. Engl.* **2021**, *60* (6), 2734-2735.

38) Zhu, Y.; Huang, D.; Wang, W.; Liu, G.; Ding, C.; Xiang, Y. *Angew. Chem., Int. Ed. Engl.* **2024**, *63* (11).

39) Kim, J.; Chen, B.; Reineke, T. M.; Li, H.; Eddaoudi, M.; Moler, D. B.; O'Keeffe, M.; Yaghi, O. M. *J. Am. Chem. Soc*. **2001**, *123*, 34, 8239–8247

40) Miura, Y.; Torres, E.; Panetta, C. A.; Metzger, R. M. *J. Org. Chem*. **1988**, *53*, 2, 439–440

41) Ise, T.; Shiomi, D.; Sato, K.; Takui, T. *Chem. Mater.* **2005**, *17*, 17, 4486–4492

42) Kim, D. J.; Oh, K. H.; Park, J. K. *Green Chem.*, **2014**,*16*, 4098-4101

APPENDIX A: INSTRUMENTAION AND DATA COLLECTION

Scanning Electron Microscopy and Energy Dispersive X-ray Spectroscopy

Scanning electron micrographs were obtained on a JEOL JSM-6460LV SEM instrument using a 515kV accelerating voltage while collecting data through the SEM Control User Interface (Version 6.21). Energy dispersive X-ray spectrographs were taken using the built in EDAX and worked up using the APEX software. SEM samples were pumped down and placed on a copper or carbon tape background followed by a gold plating process lasting 120 seconds.

Powder X-Ray Diffraction

Powder X-Ray Diffraction patterns were obtained using a Bruker D2 Phaser X-Ray Diffractometer with data collected and worked up by Dr. Diane Dickey at the University of Virginia. Powder X-Ray Diffraction patterns were also obtained using a Rigaku Miniflex with data being collected and worked up by Dr. Akhilesh Tripathi at Rigaku Americas.

Nuclear Magnetic Resonance

NMR spectra were obtained on a Jeol ECA-500 NMR for ^{1}H (500 MHz), ^{13}C (125 MHz), and ^{31}P (202 MHz).